Electronic Supplementary Material (ESI) for ChemComm.

Supporting Information section

Photo-Induced Sequence Defined Macromolecules via Hetero Bifunctional Synthons

*Nicolas Zydziak,[a,b] Florian Feist,[a,b] Birgit Huber,[a] Jan O. Mueller[a,b] and Christopher Barner-Kowollik[a,b]**

[a] Soft Matter Synthesis Laboratory, Institut für Biologische Grenzflächen, Karlsruhe Institute of Technology (KIT), Hermann-von-Helmholtz-Platz 1, 76344 Eggenstein-Leopoldshafen, Germany, christopher.barner-kowollik@kit.edu, www.macroarc.de

[b] Preparative Macromolecular Chemistry, Institut für Technische Chemie und Polymerchemie, Karlsruhe Institute of Technology (KIT), Engesserstr. 18, 76131 Karlsruhe, Germany.

Table of contents

Materials and Methods **3**

Synthesis of (2E,4E)-hexa-2,4-dien-1-yl 4-((2-formyl-3-methylphenoxy)methyl)benzoate **1** 5

Synthesis of (phenacylthio)acetic acid 2-(3,5-dioxo-10-oxa-4aza-tricyclo[5.2.1.$0^{2,6}$]dec-8-en-4-yl)ethyl ester **2** 6

Synthesis 1,6-hexanebismaleimide (**core**) 6

Synthesis of **S1** (Sequence 1) 7

Synthesis of **S2** (Sequence 2) 7

Synthesis of **S2d** (furan cleavage) 7

Synthesis of **S3** (Sequence 3) 8

Synthesis of **S4** (Sequence 4) 8

Synthesis of **S4d** (furan cleavage) 8

Synthesis of **S5** (Sequence 5) 8

Characterization of synthon 1 ..... **9**

Characterization of synthon 2 ..... **10**

Characterization of 1,6-hexanebismaleimide (core) **12**

UV-VIS spectra **15**

NMR spectroscopy tests **16**

Characterization of S1 ..... **17**

Characterization of S2 ..... **22**

Characterization of S2d **26**

Characterization of S3 ..... **29**

Characterization of S4 ..... **30**

Characterization of S4d **31**

Characterization of S5 ..... **32**

ESI-MS **33**

CID experiments of **S1** and **S2** 33

Detailed spectra of **S1**, **S2** and **S3** 36

MALDI-TOF-MS of S5 ..... **37**

SEC traces of S2d and S4d **37**

References and Notes **37**

The detailed synthesis and characterization of the reported compounds is collated in the Supporting Information section. NMR, IR and ESI-MS spectra from the starting materials, i.e. synthon **1**, **2** and 1,6-hexanebismaleimide, are found in Figure S1 to S10, as well as their respective UV spectra (Figure S11). The control experiments performed via NMR spectroscopy evidencing the stability of the reaction mixture for the first sequence in the dark at several temperatures are depicted in Figure S12. Several analyses were performed to characterize the sequence product **S1** (refer to the NMR spectra in Figure S13 to S15 and FTIR spectrum in Figure S17). The NMR spectra of the sequence products **S2** to **S5** and their assignment are reported in Figure S19 as well as in Figs. S23 to S28. For **S1** and **S2**, additional 2D NMR spectra, H-H COSY (Figure S15 and S16) and C-H HMQC (Figure S20 and S21), were recorded and enabled the assignment of the terminal and the backbone located atoms, which are of importance for the assignment for higher order sequence products. The depicted ESI-MS spectra of the core, **S1** and **S2** (respectively Figure S10, S18 and S22 as well as Table S4) confirm the success of the first and second reactions reported in the main text. Concomitantly, Collision Induced Decay (CID) experiments were performed on **S1** and **S2**, and the observed fragments proved the symmetry of the molecules (Figure S29 to S31 and Table S4). The detailed ESI-MS spectra discussed in the main text (performed under different conditions as the above cited CID experiments) for **S1**, **S2** and **S3** are found in Figure S32 and the results are collated in Table S5. Finally, the SEC traces of **S2d** and **S4d** are reported in Figure S33.

Materials and Methods

2,3-dimethylanisole (97%, Alfa Aesar), copper sulfate pentahydrate (>99%, Acros), potassium peroxodisulfate (97%, Sigma Aldrich), aluminium chloride (anhydrous, >99%, Roth), methyl-4-(bromomethyl)benzoate (97%, ABCR), 18-crown-6 (>95%, VWR), maleic anhydride (99%, Merck), furan (99%, ABCR), ethanolamine (99%, Acros), thioglycolic acid (97%, ABCR), triethylamine (≥99.5%, Sigma Aldrich), phenacyl chloride (99%, ABCR), 4-dimethyminopyridine (DMAP, ≥99%, Sigma Aldrich), *N,*N'-dicyclohexylcarbodiimide (DCC, ≥99%, Fluka), anhydrous sodium acetate (99%, Roth), acetic anhydride (≥99%, Merck), acetonitrile (>99%, Acros), sodium iodide (NaI, >99%, Merck), cetyltriethylammonium bromide (CTAB, 98%, Alpha Aesar), sodium chloride (NaCl, 99.5%, Fluka), 1,8,9-anthracenetriol (DIT, 98%, Fischer), dry *N,N*-dimethylformamide (DMF, 99.8%, Acros) and dry dichloromethane (DCM, 99.8%, Acros) were used as received. Sorbyl alcohol (98%, ABCR) was recrystallized from petroleum ether and stored under inert atmosphere at -20 °C. Tetrahydrofuran (THF), methanol (MeOH), ethanol (EtOH), diethylether (Et_2O), acetone, acetonitrile, dichloromethane (DCM) , chloroform, *n*-hexane, ethyl acetate were purchased from VWR in the highest purity. 4-((2-formyl-3-methylphenoxy)methyl)benzoic acid[1], 4-(2-hydroxyethyl)-10-oxo-4-azatricyclo[5.2.1.$0^{2,6}$]dec-8-ene-3,5-dione,[2] (phenacylthio)acetic acid[3] and 1,6-hexanebismaleimide,[4,5] were synthesized according to the literature.

Size Exclusion Chromatography (SEC)

SEC measurements were performed on a TOSOH Eco-SEC HLC-8320 GPC System, comprising an autosampler, a SDV 5 µm beadsize guard column (50 × 8 mm, PSS) followed by three SDV 5 µm columns (300 × 7.5 mm, subsequently 100 Å, 1000 Å and 10^5 Å pore size, PSS), and a differential refractive index (DRI) detector using tetrahydrofuran (THF) as the eluent at 30 °C with a flow rate of 1 mL·min^{-1}. The SEC system was calibrated using linear polystyrene standards ranging from 266 to 2.52 10^6 g·mol^{-1}. Calculation of the molecular weight proceeded via the Mark-Houwink-Sakurada (MHS) parameters for polystyrene (PS) in THF at 30 °C, i.e., K = 13.63 10^{-3} mL g^{-1}, α = 0.714.

Nuclear Magnetic Resonance (NMR) spectroscopy

^{1}H NMR sprectroscopy, H-H proton correlation spectroscopy (H-H COSY) and C-H correlation spectroscopy (Heteronuclear Multiple-Quantum Correlation, HMQC) were performed on a Bruker AM 500 spectrometer (500 MHz for ^{1}H / 125 MHz for ^{13}C). The analytes were dissolved in $CDCl_3$ and the residual solvent peaks were employed for shift correction. The following abbreviations were used to describe peak patterns when appropriate: s (singlet), d (doublet), dd (doublet of doublets), ddd (doublet of doublets of doublets), t (triplet) and m (multiplet).

Electrospray Ionization Mass-Spectrometry (ESI-MS)

ESI-MS Spectra were recorded on an LXQ mass spectrometer (Thermo-Fisher Scientific, San Jose, CA) equipped with an atmospheric pressure ionization source operating in the nebulizer assisted electrospray mode. The instrument was calibrated in the *m*/*z* range 195−1822 using a standard containing caffeine, Met-Arg-Phe-Ala acetate (MRFA) and a mixture of fluorinated phosphazenes (Ultramark 1621) (all from Aldrich). A constant spray voltage of 4.5 kV was used and nitrogen at a dimensionless sweep gas flow rate of 2 (approximately 3 L·min^{-1}) and a dimensionless sheath gas flow rate of 5 (approximately 0.5 L·min^{-1}) were applied. The capillary voltage, the tube lens offset voltage and the capillary temperature were set to 34 V, 90 V, and 275 °C respectively. The samples were dissolved with a concentration of 0.1 mg·mL^{-1} either in a mixture of THF and MeOH (3:2) containing sodium iodide at a concentration of 0.14 µg·L^{-1} (solution A), or a 0.14 µg·L^{-1} CTAB solution in DCM (solution B), and infused with a flow of 10 µL·min^{-1}. In the case of measurements performed in solution B, the molecular ion peak is identified as a cetyltriethylammonium (CTA) adduct (labelled [M-CTA]). The ionization was performed with solution A for synthon **1** and **2**, 1,6-hexanebismaleimide, **S1** and **S2**. The CID experiments for **S1** and **S2** were performed in the same conditions. However, in the main text, the presented results in Figure 5 were performed with solution B.

Fourier Transform Infrared (FTIR) spectroscopy

Infrared measurements were performed via attenuated total reflectance (ATR) using a Bruker research spectrometer VERTEX 80.

UV-VIS spectroscopy (UV-VIS)

UV-VIS spectroscopy was conducted on a Varian Cary 300 Bio spectrophotometer.

Matrix Assisted Laser Desorption Ionization – Time Of Flight Mass-Spectrometry (MALDI-TOF-MS)

The MALDI-TOF mass-spectra were recorded with an Autoflex III Smartbeam (from Bruker Daltonik GmbH, Bremen, Germany) equipped with an Nd:YAG laser (355 nm, 200 Hz). 0.5 µL of the analyte solution (1 $mg \cdot mL^{-1}$) in DCM was dropped on the target and let to dry under ambient conditions. 0.5 µL of DIT solution (50 $mmol \cdot L^{-1}$ in $HCCl_3$:EtOH 1:1) was added to the analyte on the target and let to dry under ambient conditions. 0.5 µL of saturated NaCl aqueous solution (Milli-Q water) was finally deposited and led to crystallization on the target with the analyte and DIT.

Flash chromatography

Flash chromatography was performed on an Isolera Biotage One (OS 578). The fractions were collected via a UV detector (254 nm). A SNAP Ultra (10 g) cartridge was employed for the purification in direct mode, and a SNAP C18 (12 g) cartridge for the reverse mode (both column volume of 15 mL). The analyte was dried on an adapted samplet prior to purification.

Synthesis of (2E,4E)-hexa-2,4-dien-1-yl 4-((2-formyl-3-methylphenoxy)methyl)benzoate **1**

All operations were performed under inert atmosphere. In a flame-dried Schlenk tube, 4-((2-formyl-3-methylphenoxy)methyl)benzoic acid, PE (1.71 g, 7.39 mmol, 1 eq.) and DMAP (154 mg, 1.28 mmol, 0.2 eq.) were dried overnight. Sorbyl alcohol (725 mg, 7.39 mmol, 1 eq.) was evacuated in a separate flame-dried Schlenk tube. Sorbyl alcohol was dissolved in dry DMF (3 mL) introduced via a syringe, and the obtained solution was transferred via cannula into the tube containing PE and DMAP. Dry DCM (15 mL) was added to the mixture to dissolve the components. DCC (1.69 g, 8.2 mmol, 1.3 eq.) was introduced into a separate dry Schlenk tube and evacuated. DCC was dissolved in dry DMF (5 mL) and transferred via a syringe into the solution mixture, which was cooled at 0 °C for 30 minutes. Dry DCM (17 mL) was added to the reaction mixture and stirred for 3 days at ambient temperature. After filtration and the removal of the volatiles under reduced pressure, the solid residue was dissolved in ethyl acetate and subsequently washed with 0.1 N HCl, saturated $NaHCO_3$ solution and brine. The organic phase was dried over $MgSO_4$, filtered over silica gel in DCM and dried under vacuum. The solid residue was purified by column chromatography (ethyl acetate : *n*-hexane (1:9), R_f = 0.32) after solid deposition on silica obtained from DCM. The purified compound was dried under vacuum. The reddish solution was dried under vacuum to deliver a white solid, purified via precipitation in *n*-hexane (1.53 g, 59%). ^{1}H NMR (500 MHz, $CDCl_3$): δ 10.67 (s, 1H, C*H*O), 7.41 (d, J = 8.3 Hz, 2H, Ar*H*), 7.28 (t, J = 8.0 Hz, 1H, Ar*H*), 6.77 (d, J = 8.3 Hz, 2H, Ar*H*), 6.27 (dd, J = 15.1, 10.5 Hz, 1H, CH=C*H*), 6.01 (ddd, J = 14.7, 10.5, 1.2 Hz, 1H, CH=C*H*), 5.77–5.61 (m, 2H, CH=C*H*), 5.14 (s, 2H, O–CH_2), 4.75 (d, J = 6.6 Hz, 2H, O–CH_2–CH), 2.51 (s, 3H, Ar–CH_3), 1.70 (d, J = 6.9 Hz, 3H, CH–CH_3); ^{13}C NMR (125 MHz,

$CDCl_3$): δ 192.0, 166.0, 161.9, 142.3, 141.3, 135.1, 134.4, 131.5, 130.4, 130.1, 126.8, 124.7, 123.7, 123.6, 110.3, 69.9, 65.6, 21.5, 18.2; IR (ATR, cm^{-1}): 2956, 2923, 2852, 1703, 1679, 1614, 1596, 1579, 1512, 1467, 1448, 1409, 1377, 1298, 1269, 1211, 1182, 1170, 1116, 1099, 1076, 1033, 1016, 993, 960, 921, 874, 844, 827, 804, 771, 750, 717, 680, 634, 619; ESI-MS (*m*/*z*): [**1**-Na]$^+$ calcd. for $C_{22}H_{22}O_4Na$, 373.14; found, 373.20, [**1-1**-Na]$^+$ (two adducts) calcd. for $C_{44}H_{43}O_8Na$, 722.29; found, 722.94.

Synthesis of (phenacylthio)acetic acid 2-(3,5-dioxo-10-oxa-4aza-tricyclo[5.2.1.$0^{2,6}$]dec-8-en-4-yl)ethyl ester **2**

All operations were performed under inert atmosphere. In a flame-dried Schlenk tube, (phenacylthio)acetic acid (2.00 g, 9.51 mmol, 1 eq.), 4-(2-hydroxyethyl)-10-oxo-4-azatricyclo[5.2.1.$0^{2,6}$]dec-8-ene-3,5-dione (1.99 g, 9.51 mmol, 1 eq.) and DMAP (232 mg, 1.9 mmol, 0.2 eq.) were dried overnight. Dry DMF (20 mL) was added to the reaction mixture via syringe. DCC (2.55 g, 12.36 mmol, 1.3 eq.) was evacuated in a separate flame-dried Schlenk tube, to be subsequently dissolved in dry DMF (20 mL). The DCC solution was transferred via cannula to the reaction mixture, cooled at 0 °C for 30 minutes and stirred at ambient temperature for 3 days. The reaction mixture was filtered and the volatiles removed under reduced pressure. The solid residue was dissolved in ethyl acetate and subsequently washed with 0.1 N HCl, saturated $NaHCO_3$ solution and brine. The organic phase was dried over $MgSO_4$, filtered over silica gel in DCM and dried under vacuum. The solid residue was purified by column chromatography (ethyl acetate : *n*-hexane (6:4), R_f = 0.33) after solid deposition obtained from DCM. The slightly brown solution was dried under vacuum, and the residue recrystallized from *n*-hexane : chloroform (2:1 *v*/*v*) solution to deliver a white solid (2.05 g, 5.11 mmol, 54%). ^{1}H NMR (500 MHz, $CDCl_3$): δ 7.89 (dd, J = 8.3, 1.1 Hz, 2H, Ar*H*), 7.51 (t, J = 7.4 Hz, 1H, Ar*H*), 7.40 (t, J = 7.8 Hz, 2H, Ar*H*), 6.42 (s, 2H, C=C*H*), 5.18 (s, 2H, CO–C*H*), 4.22 (t, J = 5.2Hz, 2H, O–CH_2), 3.96 (s, 2H, S–CH_2–CO), 3.71 (t, J = 5.3 Hz, 2H, N–CH_2), 3.23 (s, 2H, S–CH_2–COO), 2.80 (s, 2H, C–C*H*); ^{13}C NMR (125 MHz, $CDCl_3$): δ 193.5, 175.4, 169.1, 135.8, 134.7, 132.8, 128.0, 127.9, 80.2, 60.8, 46.8, 37.3, 37.0, 32.5; IR (ATR, cm^{-1}): 3454, 3336, 3110, 3089, 3072, 3043, 2999, 2964, 2943, 2918, 2891, 2852, 1774, 1733, 1699, 1676, 1596, 1583, 1473, 1450, 1434, 1404, 1365, 1342, 1307, 1296, 1247, 1220, 1199, 1166, 1155, 1141, 1124, 1099, 1080, 1047, 1020, 999, 960, 948, 937, 914, 877, 850, 825, 804, 779, 759, 715, 690, 651, 640, 609; ESI-MS (*m*/*z*): [**2**-Na]$^+$ calcd. for $C_{20}H_{19}NO_6SNa$, 424.08; found, 424.1, [**2-2**-Na]$^+$ (two adducts) calcd. for $C_{40}H_{38}N_2O_{12}S_2Na$, 825.18; found, 825.53.

Synthesis 1,6-hexanebismaleimide (**core**)

1,6-hexanebismaleimide was purified by column chromatography protected from light (ethyl acetate : *n*-hexane ((4: 6, R_f = 0.53), recrystallized from acetone and stored in the dark. ^{1}H NMR (500 MHz, $CDCl_3$): δ 6.62 (s, 4H, C=C–*H*), 3.43 (t, J = 7.2 Hz, 4H, N–CH_2), 1.50 (m, 4H, NCH_2–CH_2), 1.22 (m, 4H, N–C_2H_4–CH_2); ^{13}C NMR (125 MHz, $CDCl_3$): δ 170.8, 134.1, 37.7, 28.3, 26.2; IR (ATR, cm^{-1}): 3448, 3166, 3087, 2966, 2945, 2925, 2852, 1766, 1743, 1689, 1610, 1583, 1483, 1444, 1404, 1353, 1326, 1245, 1191, 1130, 1064, 1054, 1026, 954, 904, 833, 769, 736, 709, 692, 644; ESI-MS (*m*/*z*): [M-Na]$^+$ calcd. for $C_{14}H_{16}N_2O_4Na$, 299.10; found, 299.16.

Synthesis of **S1** (Sequence 1)

In a dry Schlenk round bottom flask, **1** (1.066 g, 3.04 mmol, 2 eq) and 1,6-hexanebismaleimide (525.47 mg, 1.9 mmol, 1.25 eq) were mixed and evacuated/filled with nitrogen three times. Under inert atmosphere, dry DCM (634 mL) was added and the reaction stirred in the dark until complete dissolution. Transparent vials were filled with 8 mL of the reaction mixture, sealed and kept in the dark. The solutions were purged for 10 minutes with nitrogen to be finally exposed to UV light for 45 minutes. The solutions were gathered and dried under vacuum. After purification by column chromatography (solid deposition on silica from DCM, ethyl acetate : *n*-hexane (5:5), R_f = 0.50), 1.45 g of a white solid were isolated (97.3% yield). ^{1}H NMR (500 MHz, $CDCl_3$): δ 7.94 (dd, J = 13.8, 8.1 Hz, 4H), 7.38 (d, J = 8.0 Hz, 4H), 7.12 (t, J = 7.8 Hz, 2H), 6.79 (dd, J = 7.1, 3.6 Hz, 2H), 6.71 (t, J = 7.4 Hz, 2H), 6.27 (dd, J = 14.7, 10.9 Hz, 2H), 6.06–5.92 (m, 2H), 5.88 (s, 2H), 5.79–5.58 (m, 4H), 5.12–4.94 (m, 4H), 4.81–4.61 (m, 4H), 3.58–3.35 (m, 4H), 3.17–2.96 (m, 6H), 2.96–2.82 (m, 2H), 2.77 (m, 1H), 2.61 (m, 1H), 1.70 (d, J = 6.4 Hz, 6H), 1.52 (m, 4H), 1.24 (m, 4H); ^{13}C NMR (125 MHz, $CDCl_3$, assignments referring to Figure S14): δ 180.2 (*4*), 177.7 (*15*), 166.1 (*21*), 154.7 (*11*), 141.8 (*17*), 138.7 (*7*), 135.1 (*24*), 131.5 (*23*), 130.4 (*25*), 130.0 (*26*), 129.9 (*19*), 129.6 (*9*), 126.9 (*18*), 126.2 (*12*), 123.6 (*20*), 121. (*8*), 110.8 (*10*), 69.8 (*16*), 65.5 (*22*), 61.1 (*13*), 46.6 (*14*), 38.6 (*5*), 38.2 (*3*), 27.8 (*6*), 27.2 (*2*), 25.7 (*1*), 18.2 (*27*); IR (ATR, cm^{-1}): 3450, 3022, 2927, 2854, 1770, 1691, 1674, 1606, 1587, 1510, 1470, 1439, 1404, 1371, 1348, 1300, 1271, 1174, 1151, 1107, 1053, 1018, 989, 958, 918, 875, 844, 821, 789, 754, 731, 692, 665, 650, 621; ESI-MS (*m*/*z*): [**S1**-Na]$^+$ calcd. for $C_{58}H_{60}N_2O_{12}Na$, 999.40; found, 999.48, and [**S1**-CTA]$^+$ calcd. for $C_{77}H_{102}N_3O_{12}$, 1260.75; found, 1260.34 (under CTAB ionization conditions).

Synthesis of **S2** (Sequence 2)

The reaction was conducted similarly to the synthesis of **S1**, except that the reagent **S1** (148.0 mg, 151.4 µmol, 1 eq) and **2** (180.3 mg, 536.0 µmol, 3 eq) were dissolved in 80 mL of dry DCM. The purification was conducted via column chromatography (ethyl acetate : *n*-hexane (5:5)), after solid deposition from DCM, to eliminate photochemically released acetophenone. With a ternary eluent (ethyl acetate : *n*-hexane : MeOH 45.5:45.5:9), **S2** was isolated (R_f = 0.23) to deliver a slight yellowish solid (36% yield). ESI-MS (*m*/*z*): [**S2**-Na]$^+$ calcd. for $C_{82}H_{82}N_4O_{22}S_2Na$, 1561.48; found, 1561.32, and [**S2**-CTA]$^+$ calcd. for $C_{101}H_{124}N_5O_{22}S_2$, 1822.82; found, 1822.72 (under CTAB ionization conditions).

Synthesis of **S2d** (furan cleavage)

Under inert atmosphere and protected from light, **S2** was dissolved in cyclohexane and heated at 80 °C for 3 days. After evaporation under vacuum, the residue was additionally heated at 80 °C for 24 h, under vacuum and protected from light. The purification was conducted via flash chromatography with ethyl acetate : *n*-hexane (5:5), and a MeOH gradient (1% per 10 column volume, 10 mL·min^{-1}). The product was eluted as the MeOH content reached 3 to 4% in the mobile phase and dried to deliver a white solid (41% yield, R_f = 0.43 in ethyl acetate : *n*-hexane : MeOH 45.5:45.5:9).

Synthesis of **S3** (Sequence 3)
Similarly to compound **S1**, **S2d** was led to react with **1** in dry DCM. The purification was performed via flash chromatography with ethyl acetate : *n*-hexane (5:5), and a MeOH gradient (1% per 10 column volumes, 10 mL·min^{-1}). The product was eluted as the MeOH content reached 0 to 3% in the mobile phase and dried to deliver a white solid (59% yield). ESI-MS (*m*/*z*): [**S3**-CTA]$^+$ calcd. for $C_{137}H_{160}N_5O_{28}S_2$, 2387.07; found, 2386.86 (under CTAB ionization conditions).

Synthesis of **S4** (Sequence 4)
Similarly to compound **S2**, **S3** was led to react with **2** in dry DCM. The purification was performed via reverse phase flash chromatography with MeOH and a DCM gradient (2.4% per 10 column volumes, 10 mL·min^{-1}). The product was eluted as the DCM content reached 16 to 32% in the mobile phase (52% yield).

Synthesis of **S4d** (furan cleavage)
The deprotection was performed under similarly as for compound **S2d**. The purification was performed via reverse phase flash chromatography with MeOH and a DCM gradient (10% per 4 column volumes, 10 mL·min^{-1}). The product was eluted as the DCM content reached 0 to 10% in the mobile phase (58% yield).

Synthesis of **S5** (Sequence 5)
Similarly to compound **S2**, **S4d** was led to react with **1** in dry DCM. The purification was performed via reverse phase flash chromatography with MeOH and a DCM gradient (2.5% per 4 column volumes, 10 mL·min^{-1}). The product was eluted as the DCM content reached 0 to 10% in the mobile phase (47% yield). MALDI-TOF-MS (*m*/*z*): [**S5**-Na]$^+$ calcd. for $C_{178}H_{176}N_6O_{44}S_4Na$, 3253.05; found, 3253.05.

Table S1. Collation of the experimental conditions for the generation of **S1** to **S5** at ambient temperature at 350 nm (λ_{max}), in dry DCM. The concentration is provided for the core and the sequential starting material.

Sequence product	Ligation of	Reactant ratio	*c* / 10^{-3} mol·L^{-1}	*t* / min
S1	**core+1**	1.25 : 2	3.00	45
S2	**S1+2**	1 : 3	1.89	45
S3	**S2d+1**	1 : 2	0.83	45
S4	**S3+2**	1 : 3	0.83	45
S5	**S4d+1**	1 : 2	0.83	45

Characterization of synthon 1

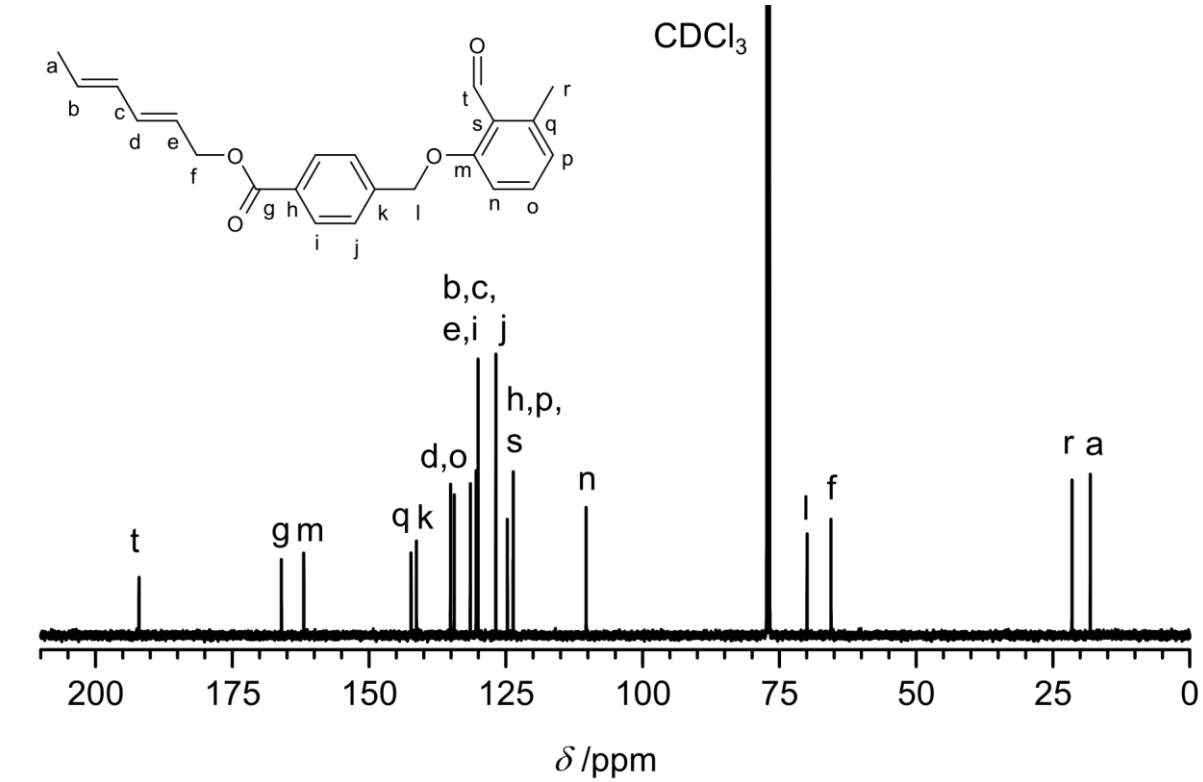

Figure S1. ^{13}C NMR spectrum of synthon **1** (125 MHz, $CDCl_3$).

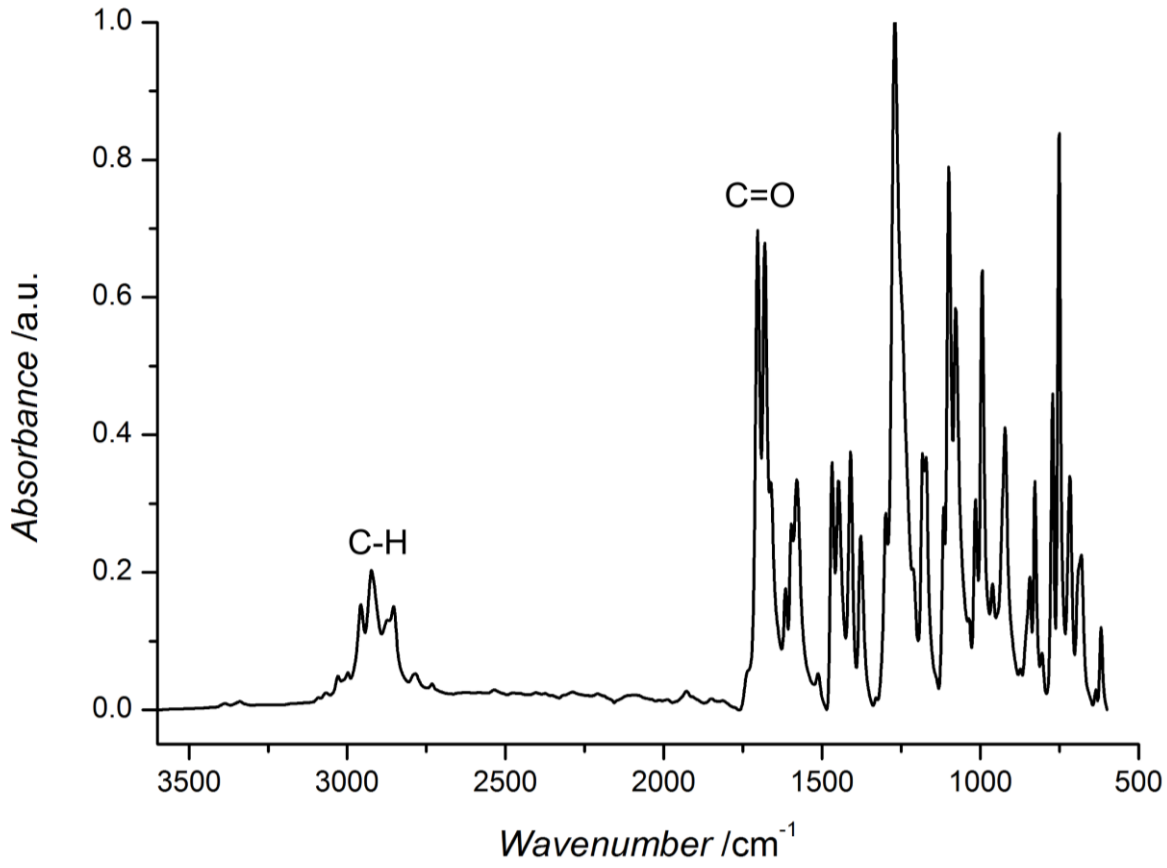

Figure S2. FTIR (ATR) spectrum of synthon **1**.

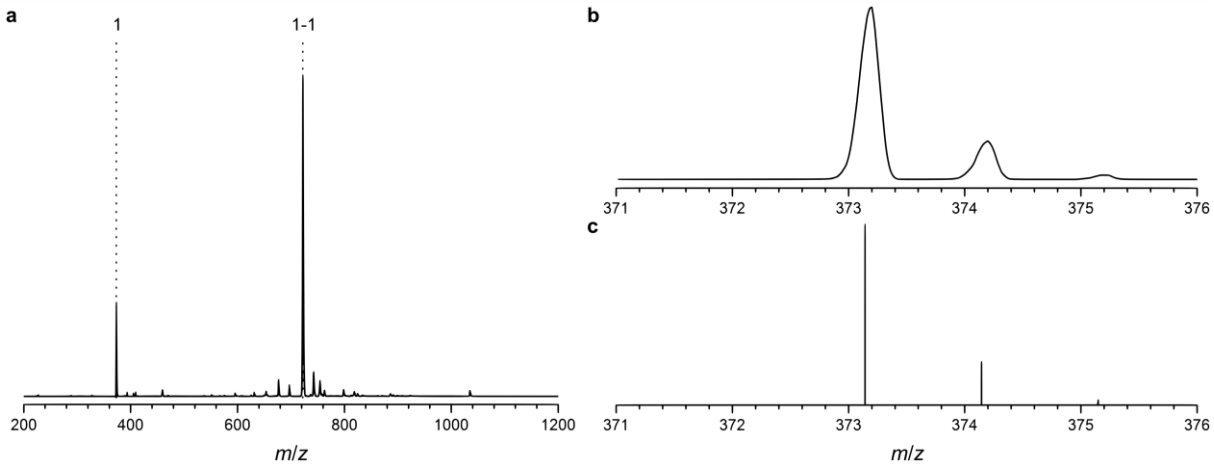

Figure S3. ESI-MS spectrum of compound **1** (a, one adduct [**1**-Na]$^+$ at 373.20 *m/z*, two adducts [**1-1**-Na]$^+$ at 722.94 *m/z*). The detailed (b) and predictable (c) spectra are shown too (solvent A conditions, sodium adducts).

Characterization of synthon 2

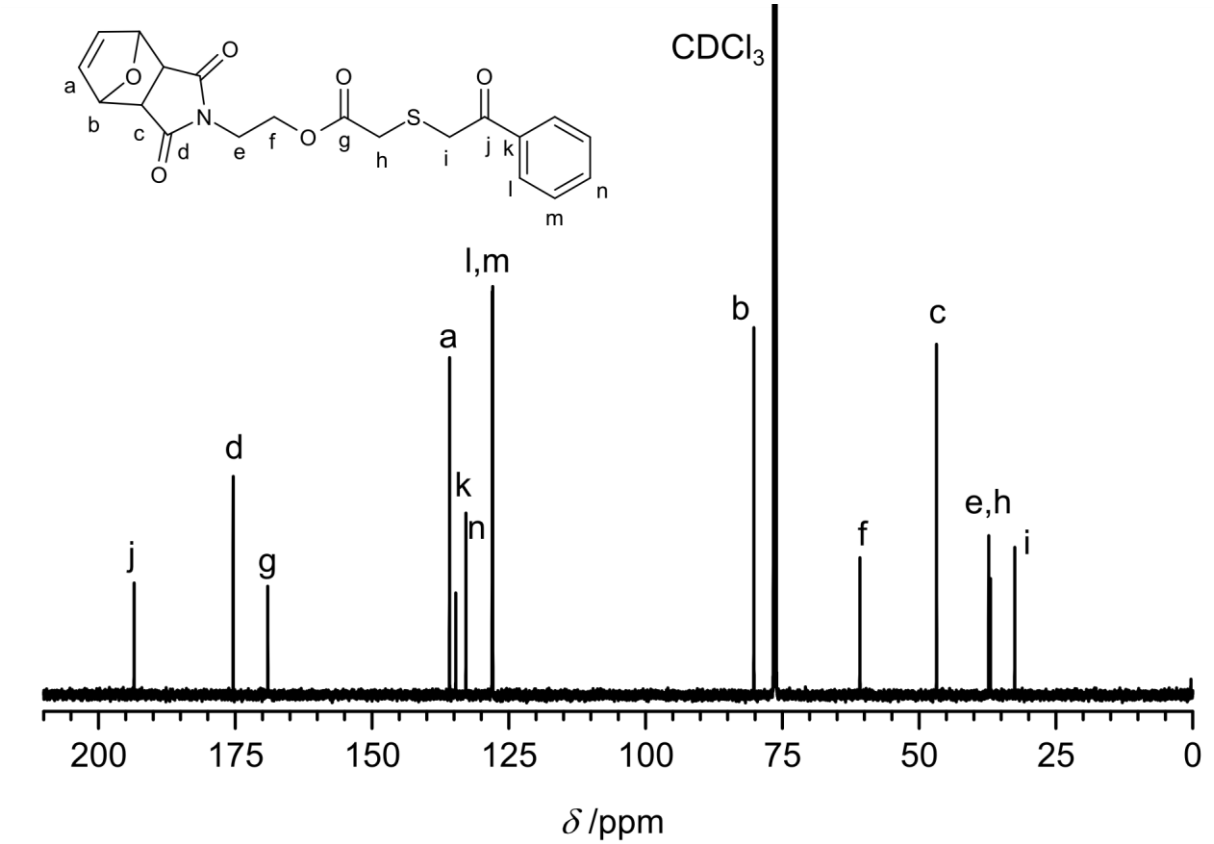

Figure S4. ^{13}C NMR spectrum of synthon **2** (125 MHz, $CDCl_3$).

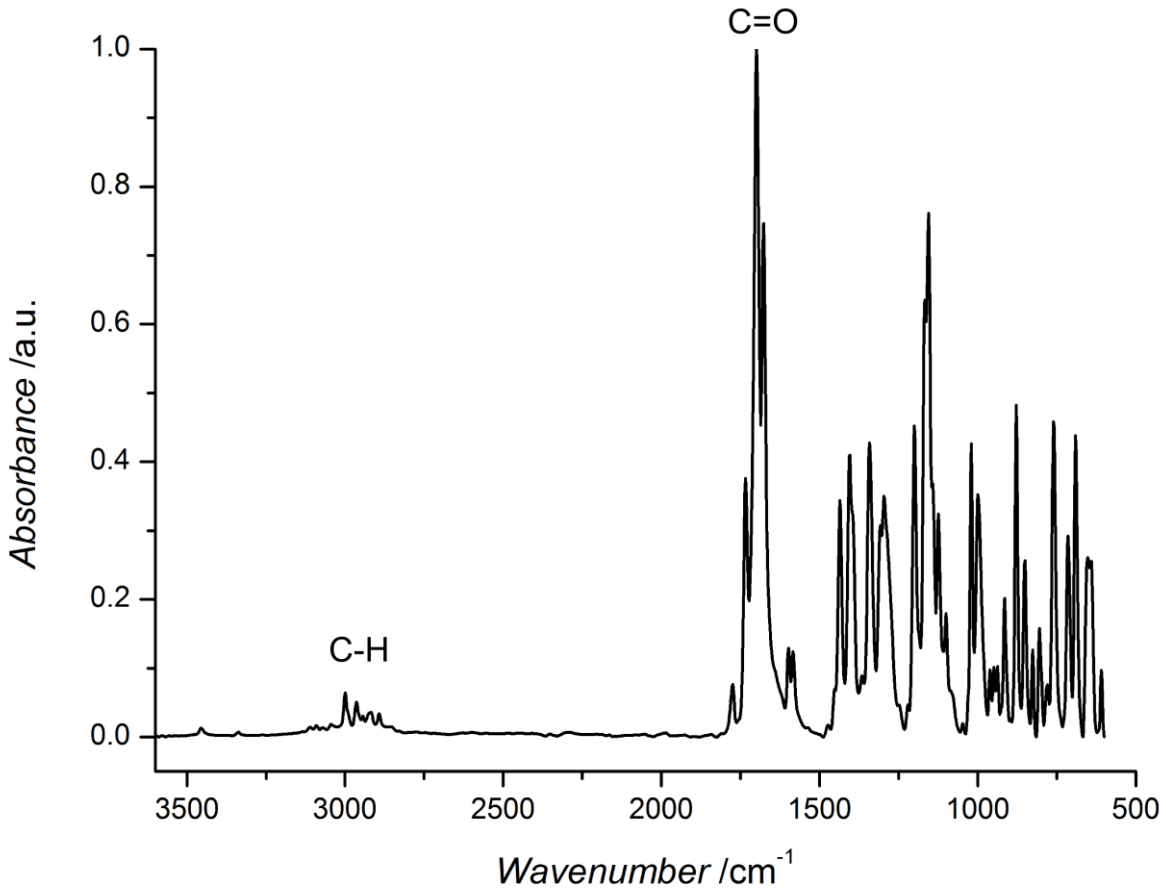

Figure S5. FTIR (ATR) spectrum of synthon **2**.

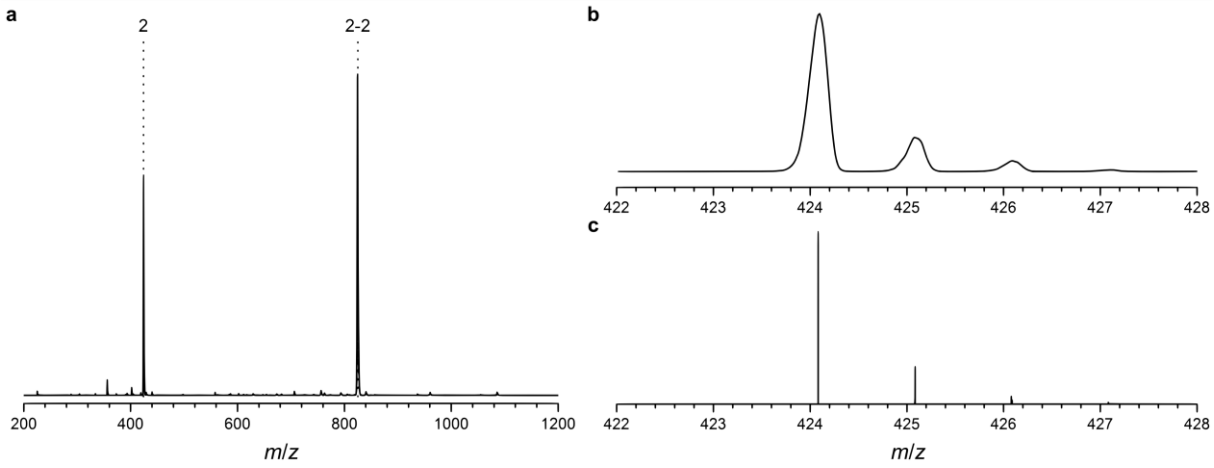

Figure S6. ESI-MS spectrum of compound **2** (a, one adduct [**2**-Na]$^+$ at 421.10 *m*/*z*, two adducts [**2-2**-Na]$^+$ at 824.53 *m*/*z*). The detailed (b) and predictable (c) spectra are shown too (solvent A conditions, sodium adducts).

Characterization of 1,6-hexanebismaleimide (core)

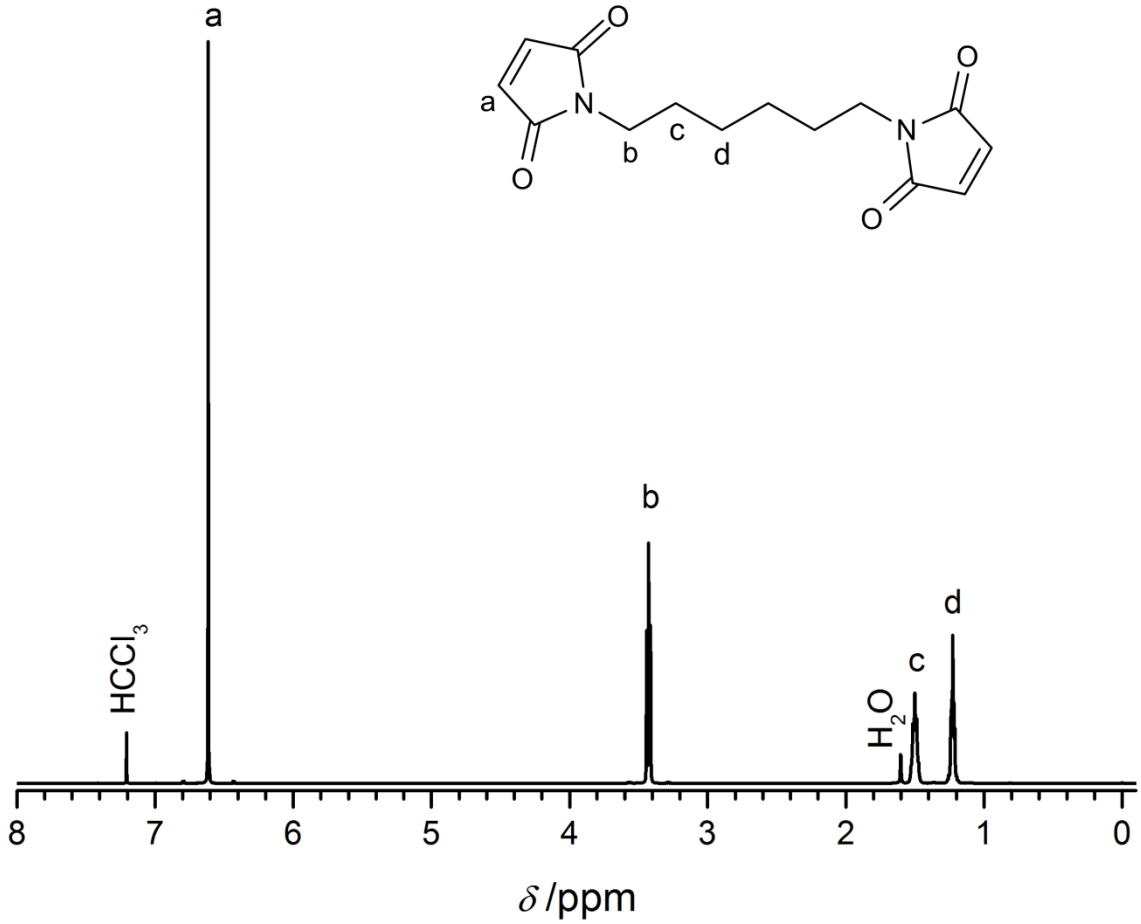

Figure S7. ^{1}H NMR spectrum of 1,6-hexanebismaleimide (core) (500 MHz, $CDCl_3$).

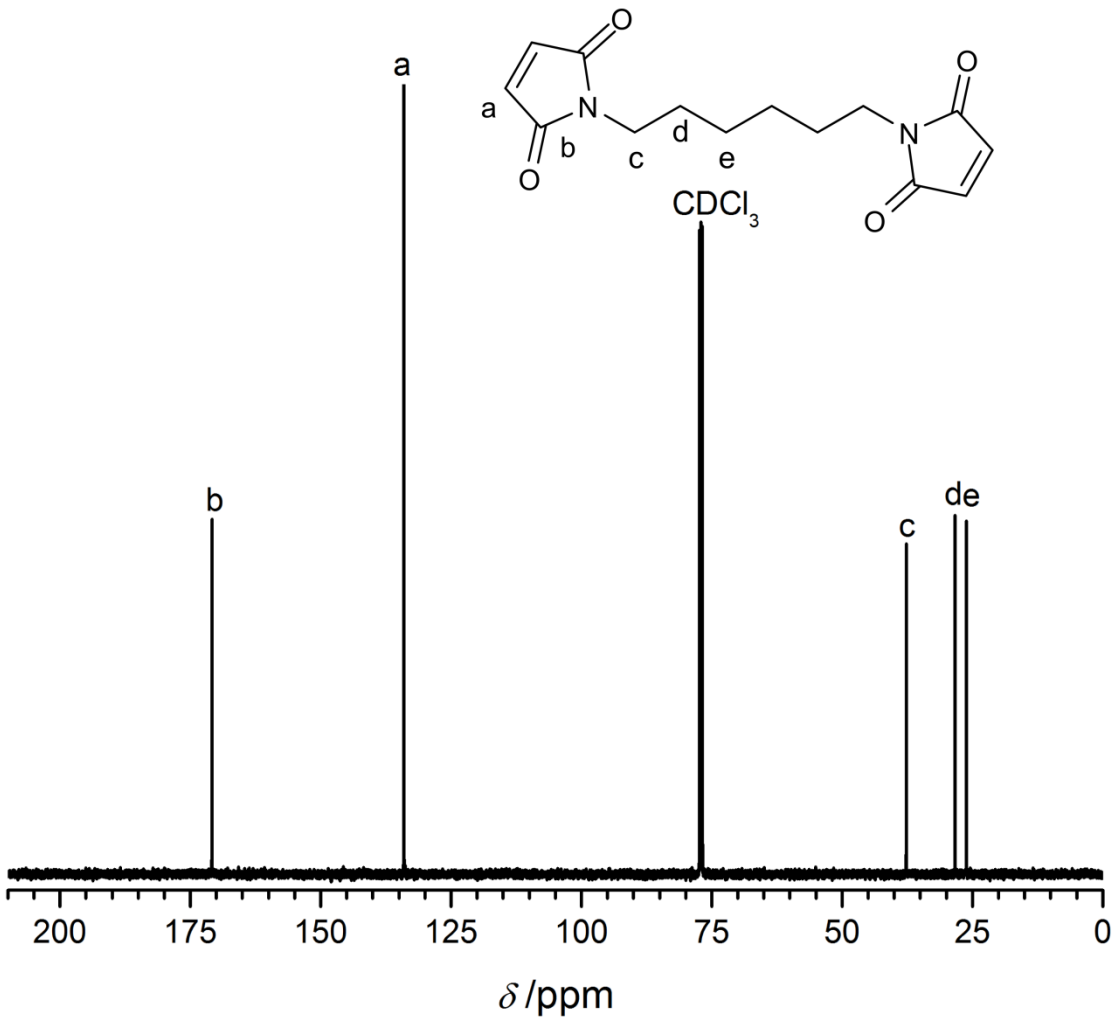

Figure S8. ^{13}C NMR spectrum of 1,6-hexanebismaleimide (core) (125 MHz, $CDCl_3$).

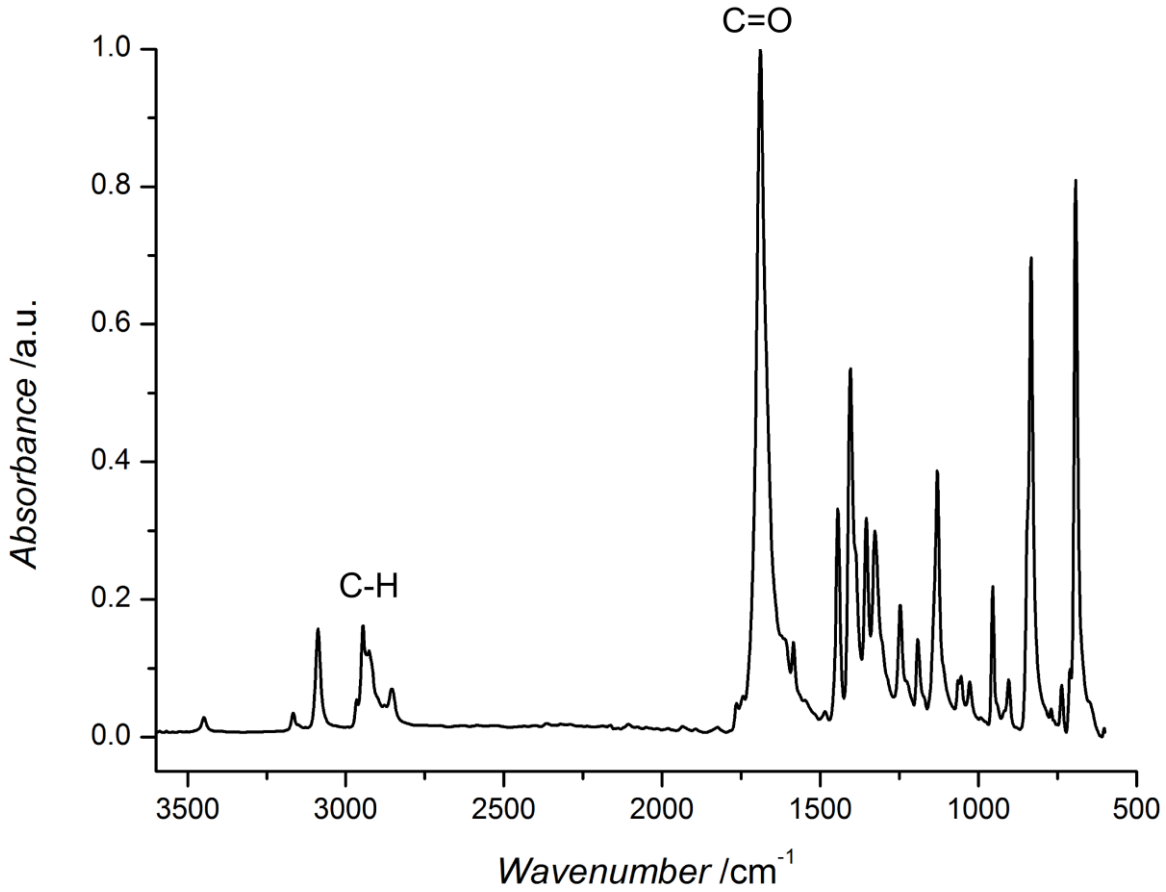

Figure S9. FTIR (ATR) spectrum of 1,6-hexanebismaleimide (core).

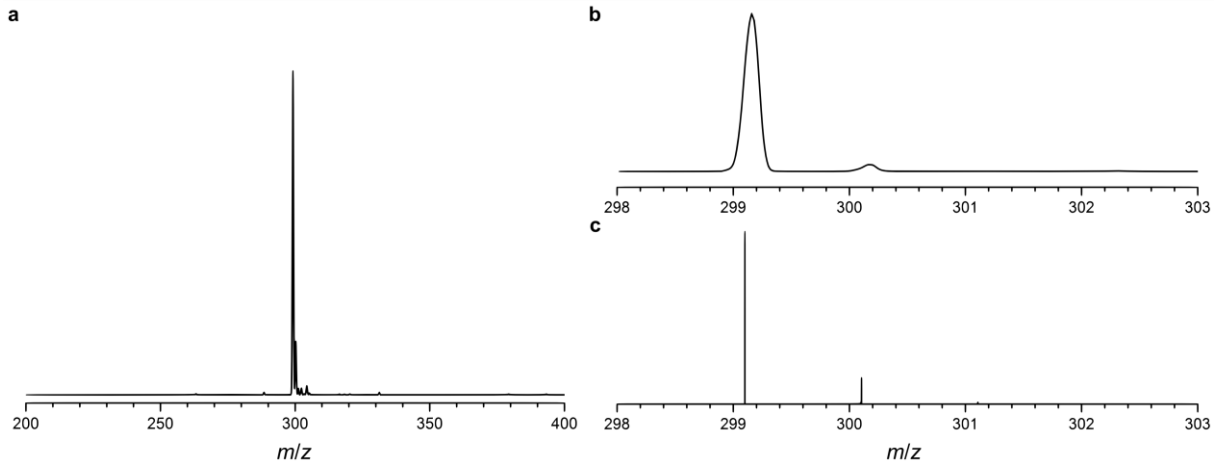

Figure S10. ESI-MS spectrum of 1,6-hexanebismaleimide (a, one sodium adduct at 299.16 *m*/*z*). The detailed (b) and predictable (c) spectra are shown too (solvent A conditions, sodium adducts).

UV-VIS spectra

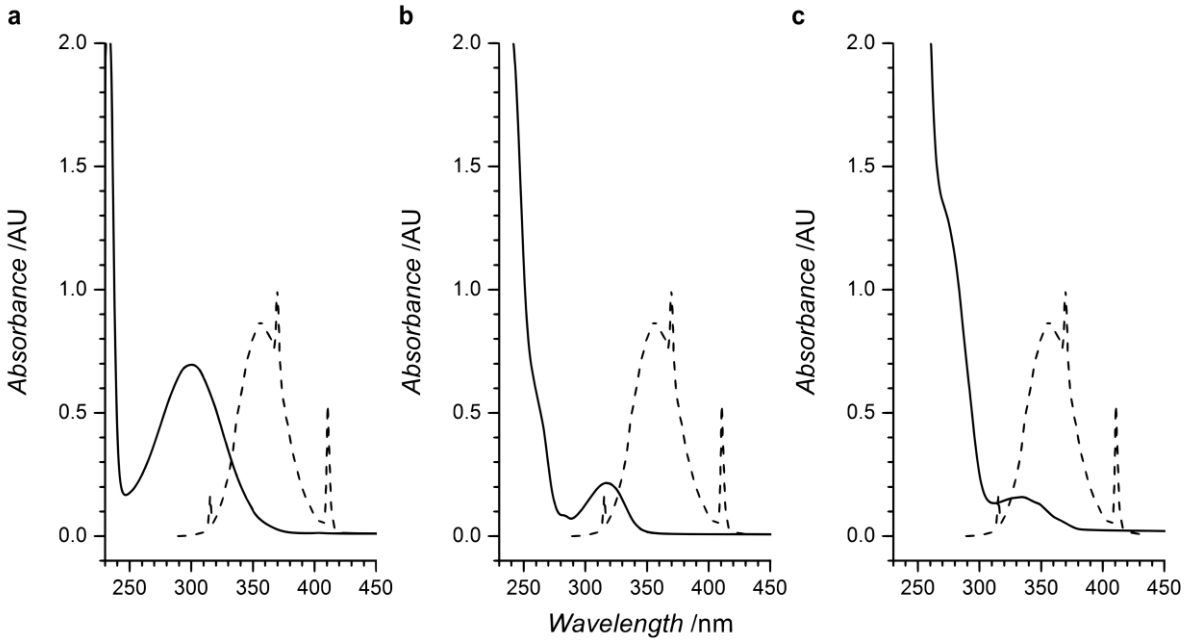

Figure S11. UV-VIS spectra of 1,6-hexanebismaleimide (core, a) and synthon **1** (b) and **2** (c) in acetonitrile. The emission spectrum of the employed lamp for the sequential reactions is depicted in each spectrum.

NMR spectroscopy tests (assessment of sorbyl groups thermal stability)

The control experiments performed via NMR spectroscopy evidencing the stability of the reaction mixture for the first sequence, in the dark at several temperatures, is depicted in Figure S12. No changes in the spectra of the reaction mixture (spectrum d) are observed when the samples is stored in the dark, for 24h (spectrum c), or exposed to 40 °C (spectrum b) or 60 °C (spectrum a) for 1h in the dark.

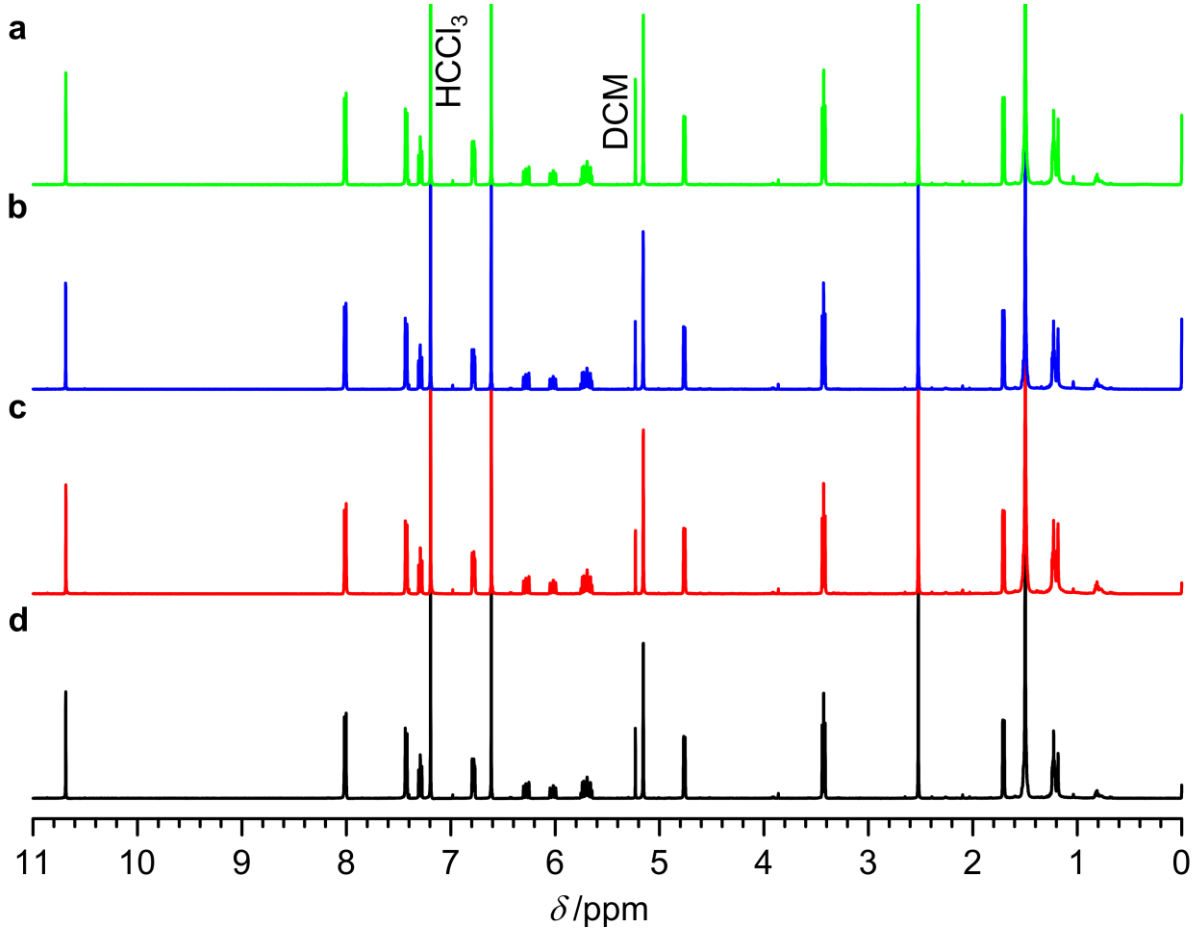

Figure S12. ^{1}H NMR spectra of the reaction mixture in dry DCM for the first sequence stored in the dark: at t_0 (a), after 24h (b), after 1h at 40 °C (c) and 60 °C (d) (500 MHz, $CDCl_3$).

Characterization of S1

The interpretation of ^{13}C NMR spectrum was enabled by 2D NMR (H-H COSY and C-H HMQC).

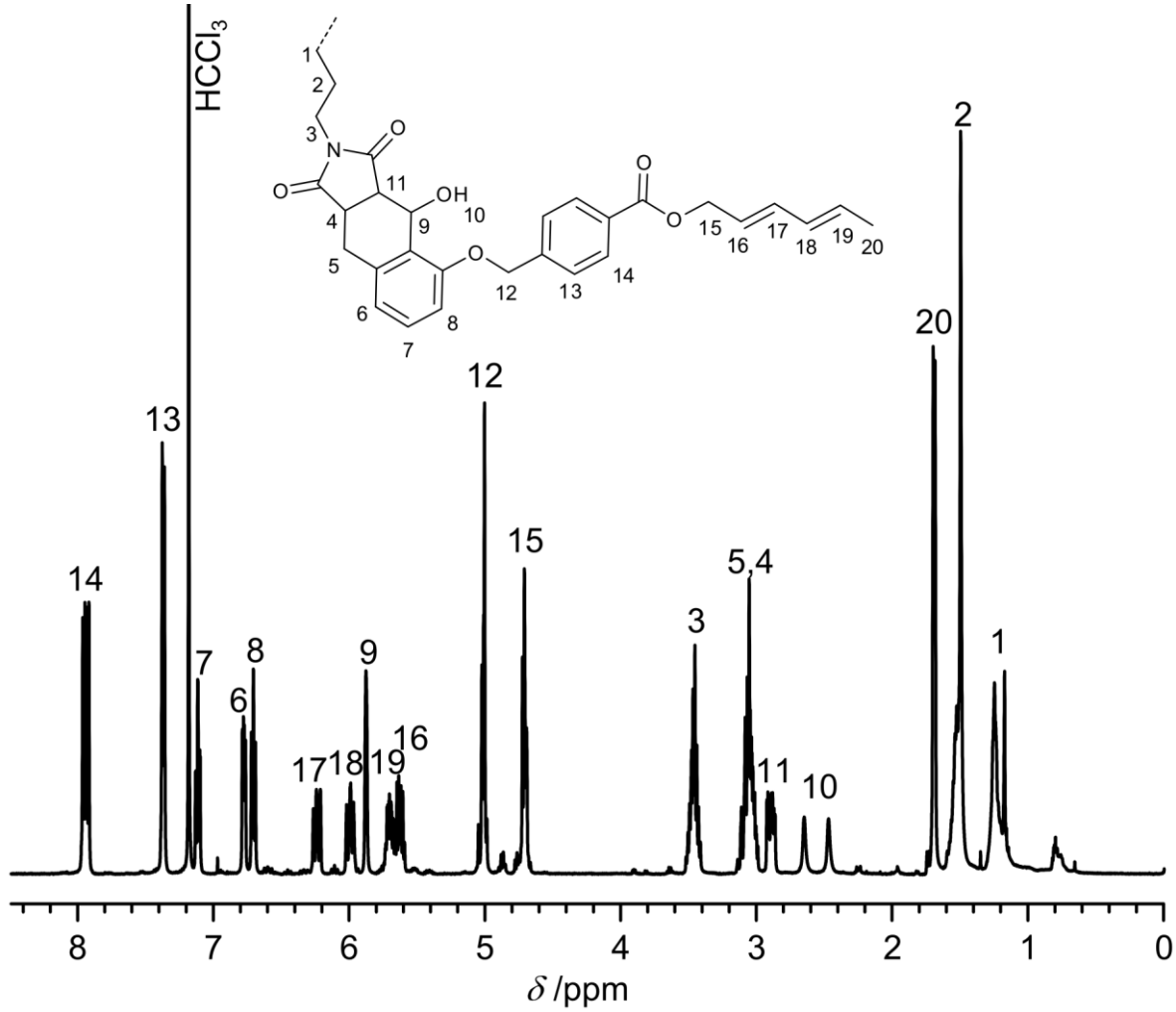

Figure S13. ^{1}H NMR spectrum of **S1** (500 MHz, $CDCl_3$).

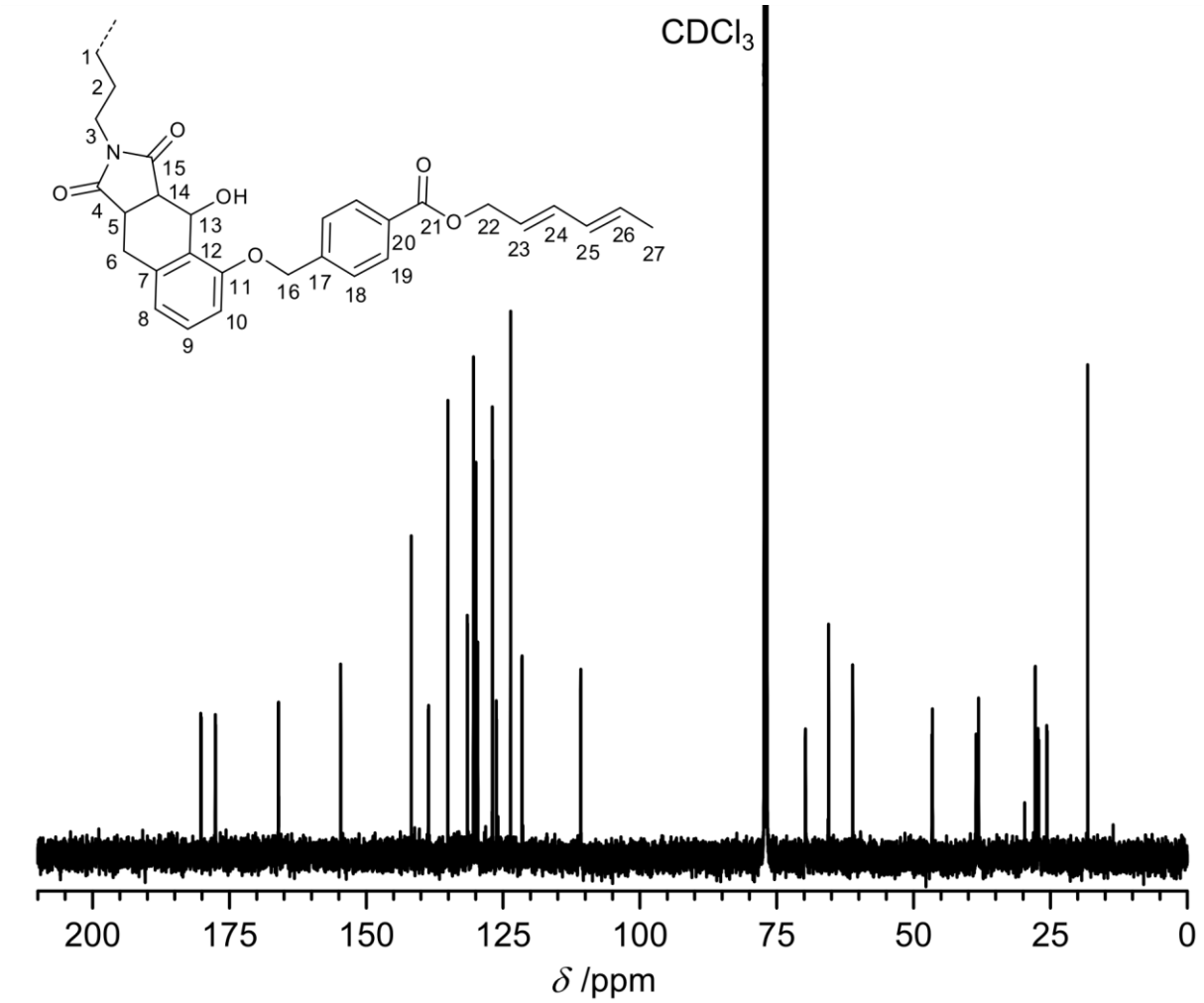

Figure S14. ^{13}C NMR spectrum of **S1** (125 MHz, $CDCl_3$).

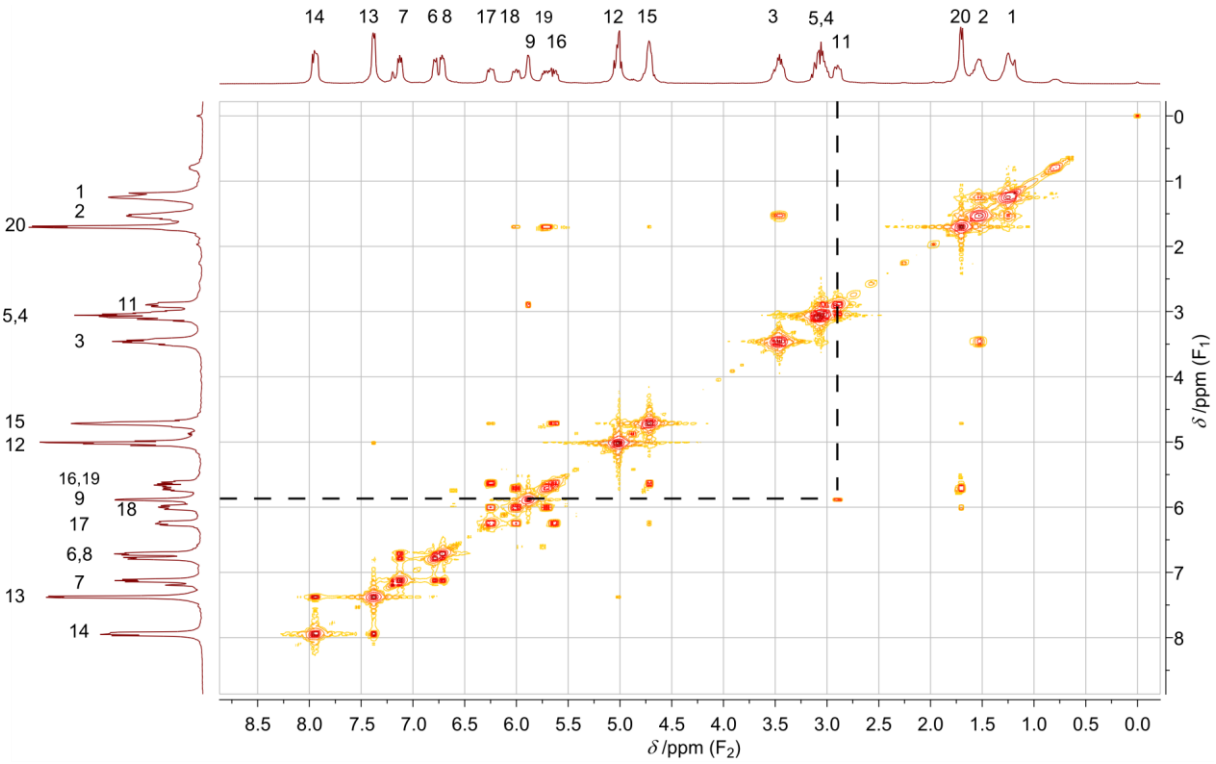

Figure S15. H-H COSY NMR spectrum of **S1** ($CDCl_3$). The correlated protons *9* and *11* representative of the new covalent bond are highlighted (proton assignment identical as in Figure S13).

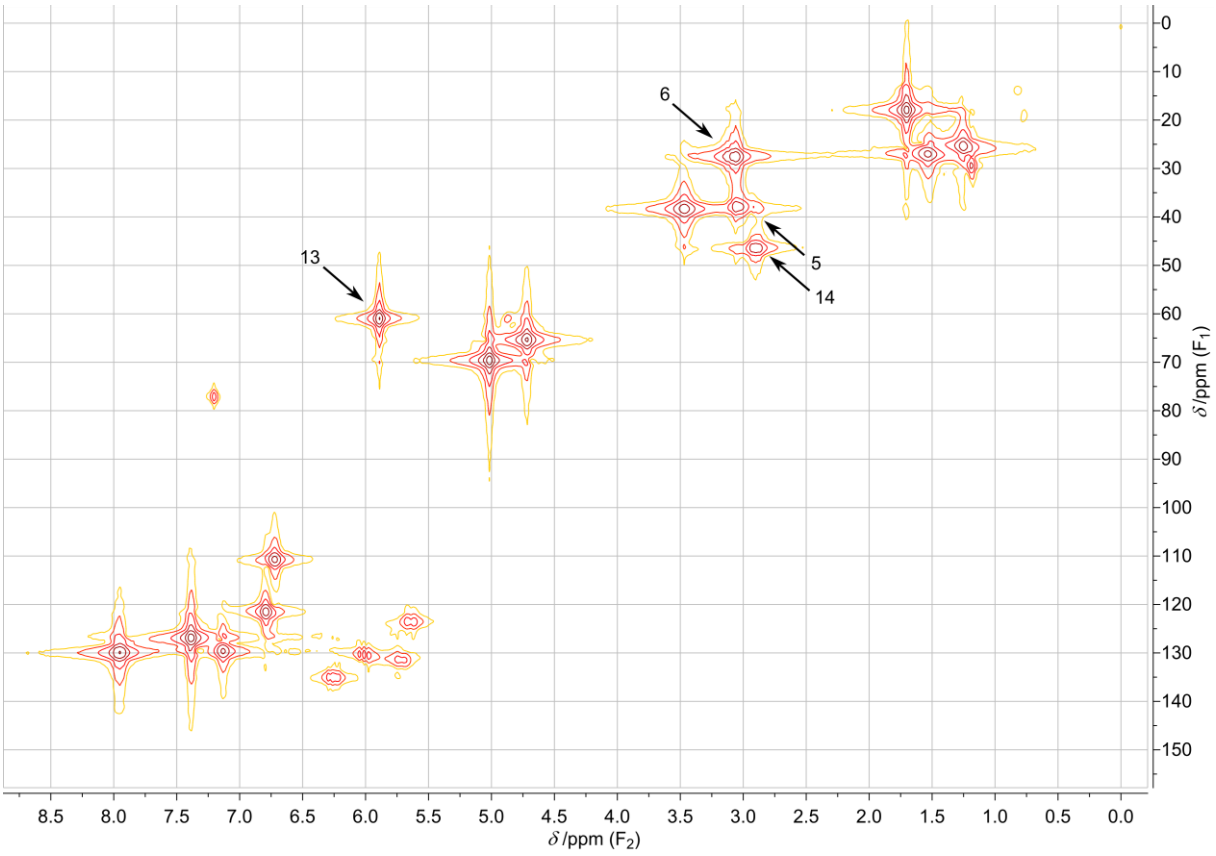

Figure S16. C-H HMQC NMR spectrum of **S1** ($CDCl_3$). The carbon atoms *5*, *6*, *13* and *14* representative of the new covalent bond are highlighted (atom assignment identical as in Figure S14).

The detection of OH bond signals at 3500 cm^{-1} via infrared spectroscopy evidences the successful reaction between the synthon **1** and 1,6-hexanebismaleimide.

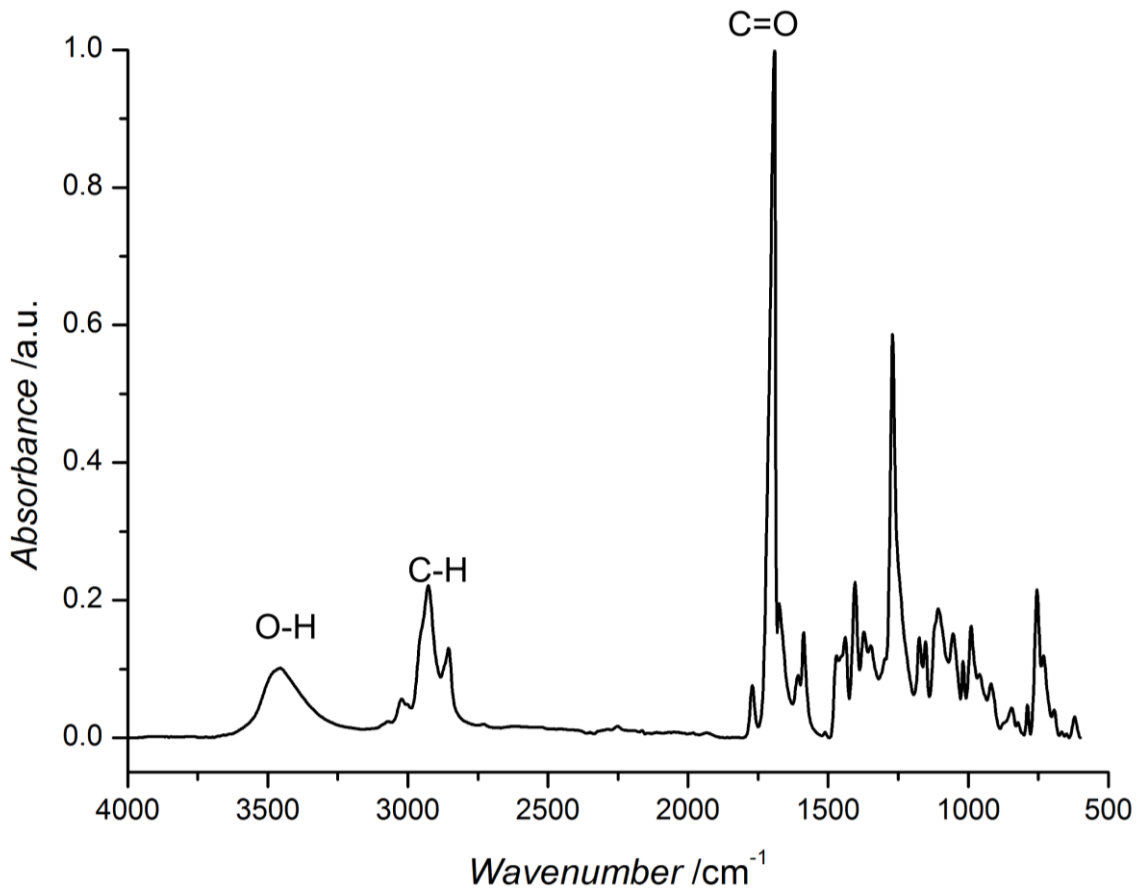

Figure S17. FTIR (ATR) spectrum of **S1**.

The observed *m*/*z*-shift of the core (1,6-hexanebismaleimide), located at 299.16 *m*/*z*, to the product **S1**, located at 999.48 *m*/*z* corresponds to the *m*/*z* shift predicted by the addition of two molecules of **1** to the core (+700.32 *m*/*z*).

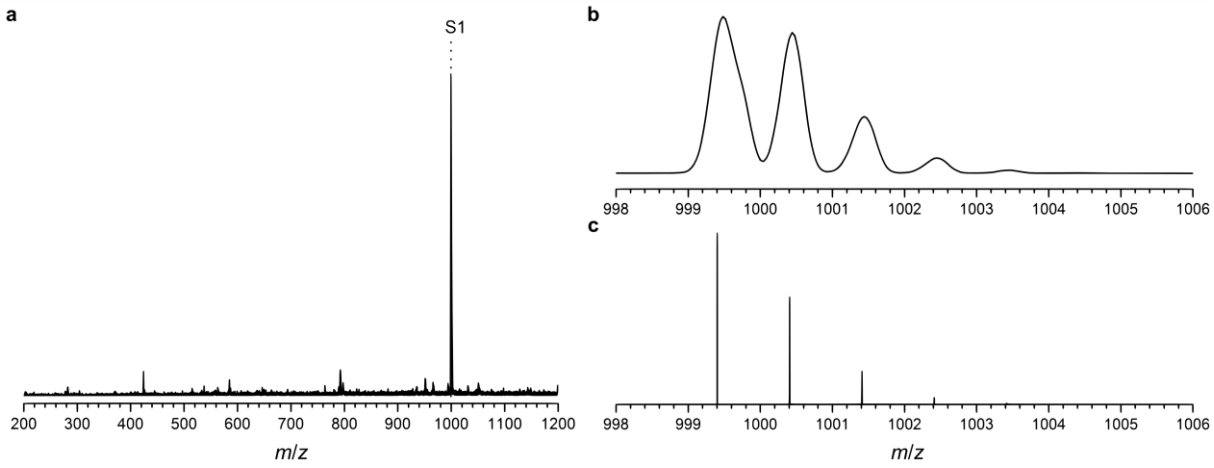

Figure S18. ESI-MS spectrum of compound **S1** (a, one adduct [**S1**-Na]$^{+}$ at 999.48 *m*/*z*). The detailed (b) and predictable (c) spectra are shown too (solvent A conditions, sodium adducts).

Characterization of S2

The ^{1}H spectrum was recorded in $CDCl_3$ delivering similar shifts of the proton resonances constituting the backbone as for **S1** (protons *1* to *14*), with shifted and additional signals for the protons *15* to *26*, and the additional protons related to the reaction with **2**. A similar method was performed for the carbon assignments, showing chemical shifts and additional signals for the carbons *22* to *35*. The assignment of the chemical shifts was enabled by 2D NMR (H-H COSY and C-H HMQC). Only the chemical shifts of carbon atoms bonded with a proton could be recorded due to the use of C-H HMQC experiments.

Table S2. Summary of modified signals from the ^{1}H and ^{13}C NMR spectroscopy of **S2**.

	Atom number	Shifted signal (δ /ppm)	New signal (δ /ppm)
H 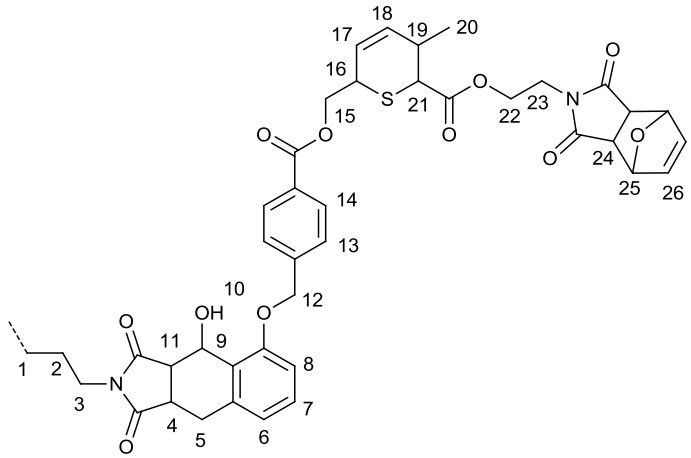	15	4.43	-
	16	2.91	-
	17	5.67	-
	18	5.87	-
	19	3.61	-
	20	1.28	-
	21	3.76	-
	22	-	4.31
	23	-	3.79
	24	-	2.79
	25	-	5.24
	26	-	6.43
C 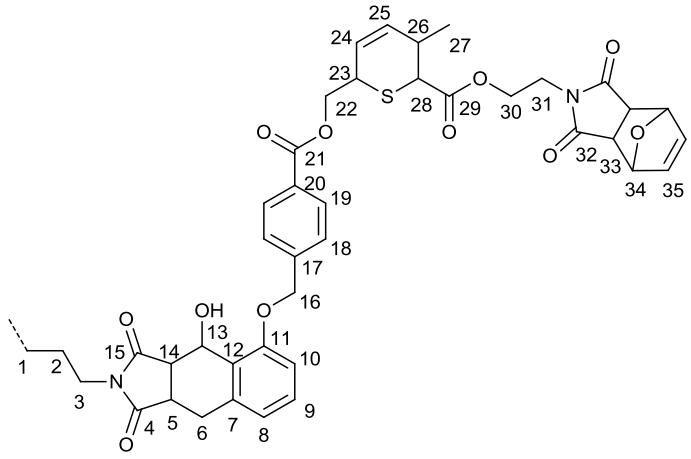	22	66.2	-
	23	34.9	-
	24	124.3	-
	25	133.4	-
	26	31.5	-
	27	20.4	-
	28	41.3	-
	30	-	61.3
	31	-	37.0
	33	-	47.5
	34	-	80.9
	35	-	135.8

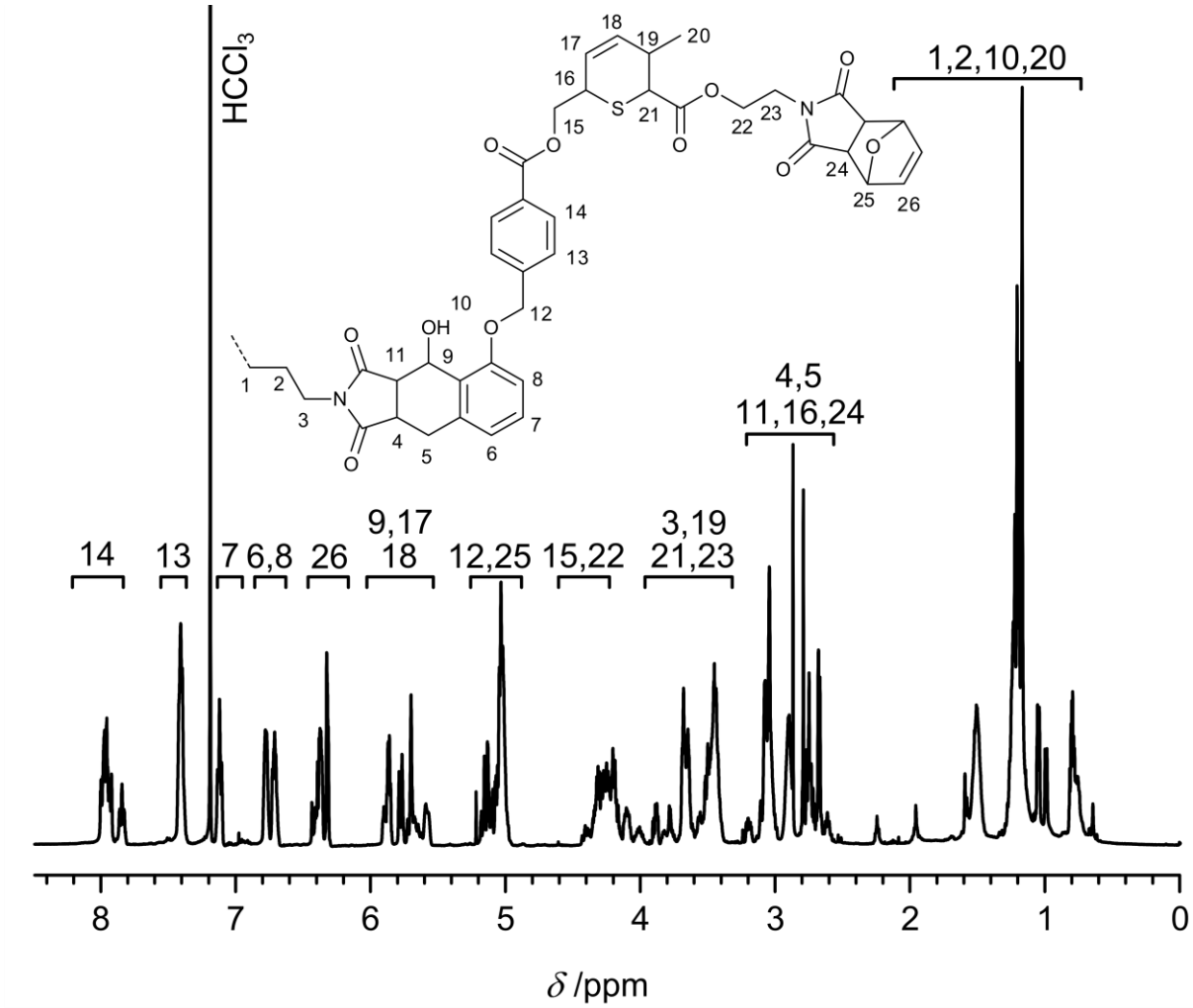

Figure S19. ^{1}H NMR spectrum of **S2** (500 MHz, $CDCl_3$).

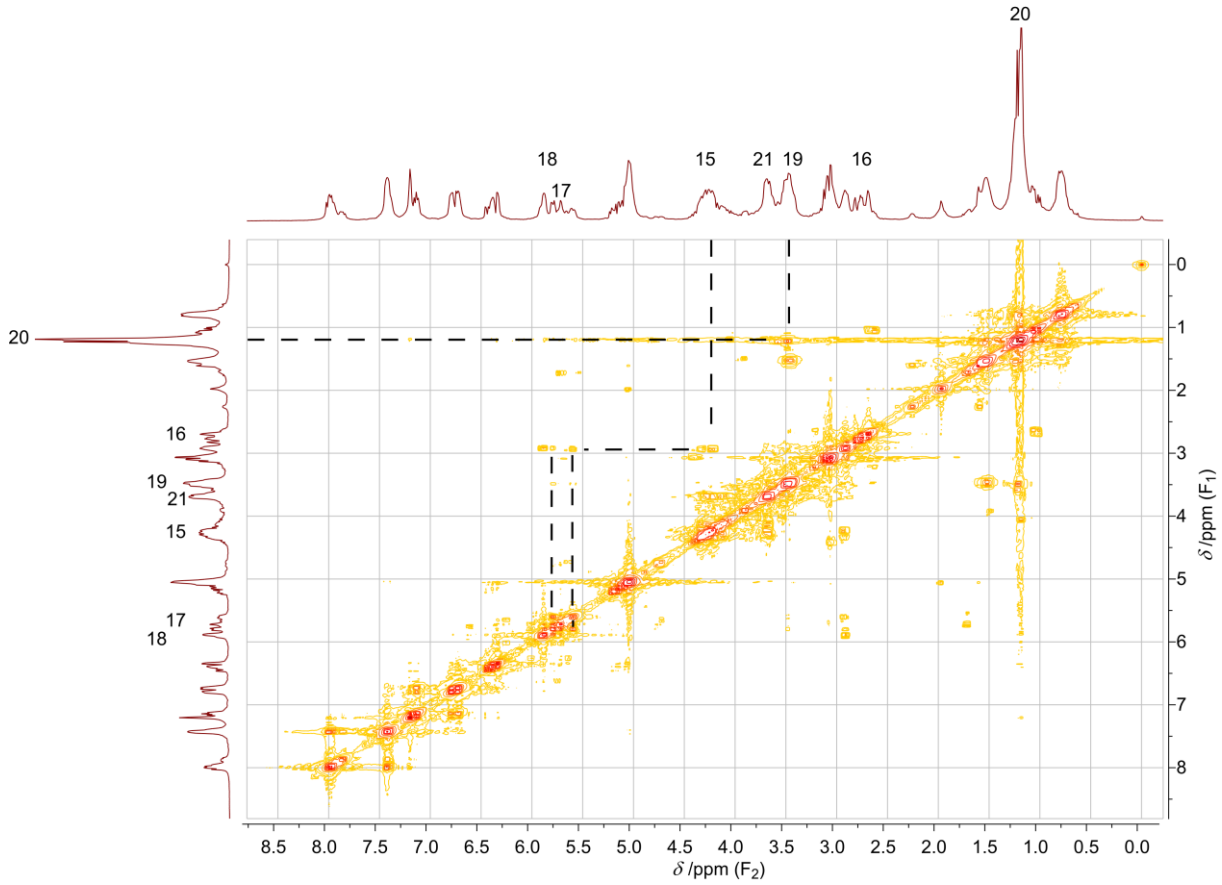

Figure S20. H-H COSY NMR spectrum of **S2** ($CDCl_3$). The correlated protons *15* to *21* representative of the new covalent bond are highlighted (proton assignment identical as in Figure S19).

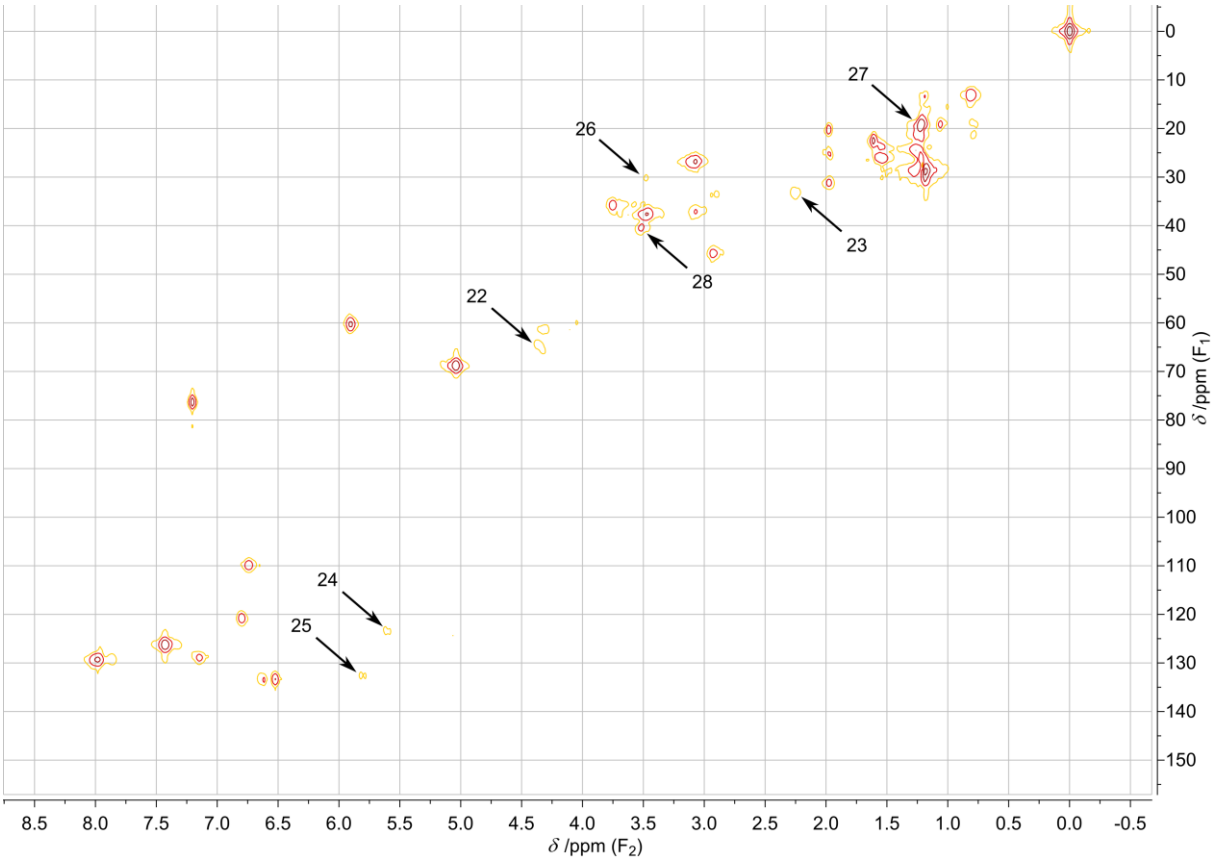

Figure S21. C-H HMQC NMR spectrum of **S2** ($CDCl_3$). The carbon atoms *22* and *28* representative of the new covalent bond are highlighted (atom assignment identical as in Table S2).

The observed *m/z*-shift of **S1** (1,6-hexanebismaleimide), located at 999.48 *m/z*, to **S2**, located at 1561.32 *m/z* corresponds to the *m/z* shift predicted by the addition of two fragments of **2** (+561.84 *m/z*).

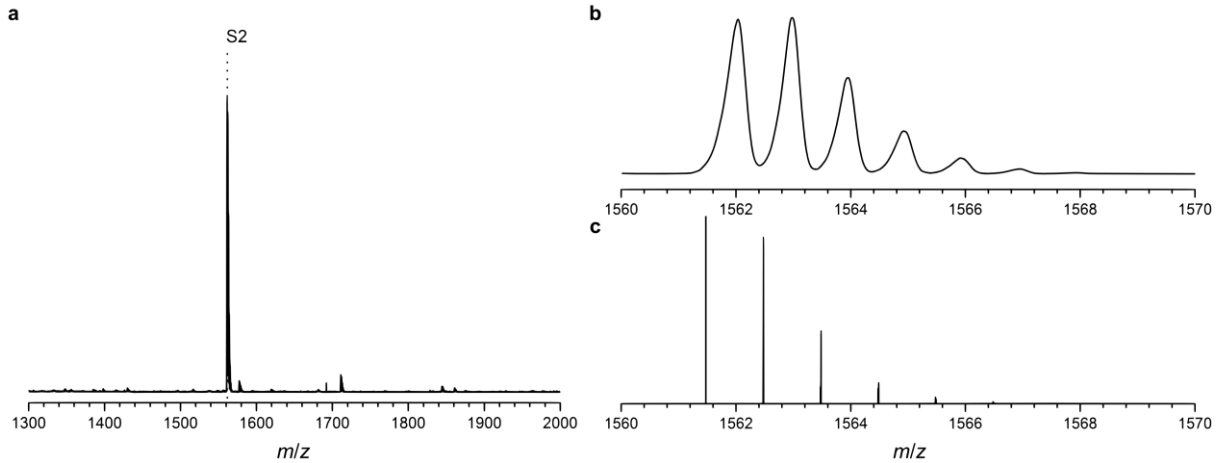

Figure S22. ESI-MS spectrum of **S2** (one adduct [**S2**-Na]$^+$ at 1561.32 *m/z*). The detailed (b) and predictable (c) spectra are shown too (solvent A conditions, sodium adducts).

Characterization of S2d

^{1}H and ^{13}C NMR spectra recorded in $CDCl_3$ depict similarities with the spectra of **S2** with changes in chemical shifts for the proton *24* and the carbon *33*, due to the cleavage of the furan moiety. Signals related to furan disappeared (protons *25* and *26*, carbons *24* and *35*). The assignment of the chemical shifts was enabled by 2D NMR (H-H COSY and C-H HMQC). Only the chemical shifts of carbon atoms bonded with a proton could be recorded due to the use of C-H HMQC experiments.

Table S3. Summary of modified signals from the ^{1}H and ^{13}C NMR spectroscopy of **S2d**.

		Atom number	Shifted signal (δ /ppm)
H	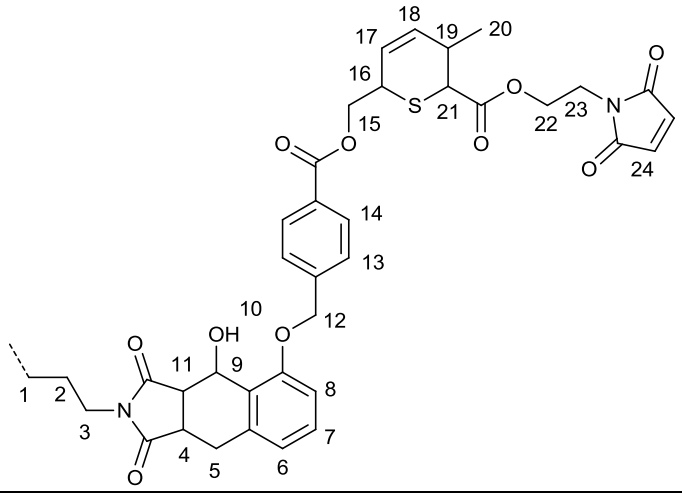	24	6.60
C	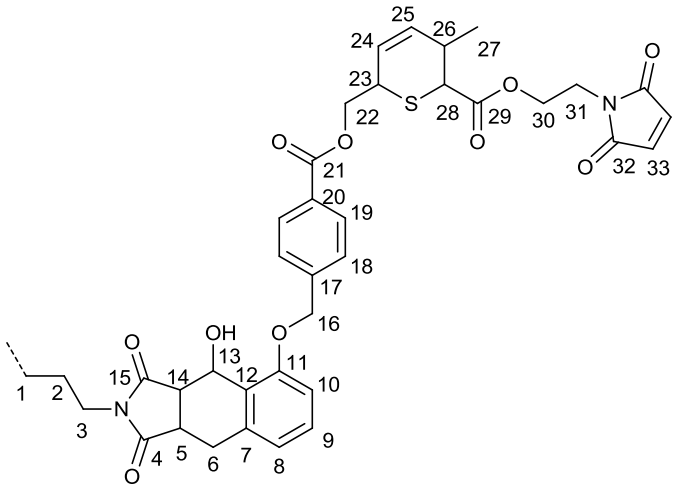	33	134.1

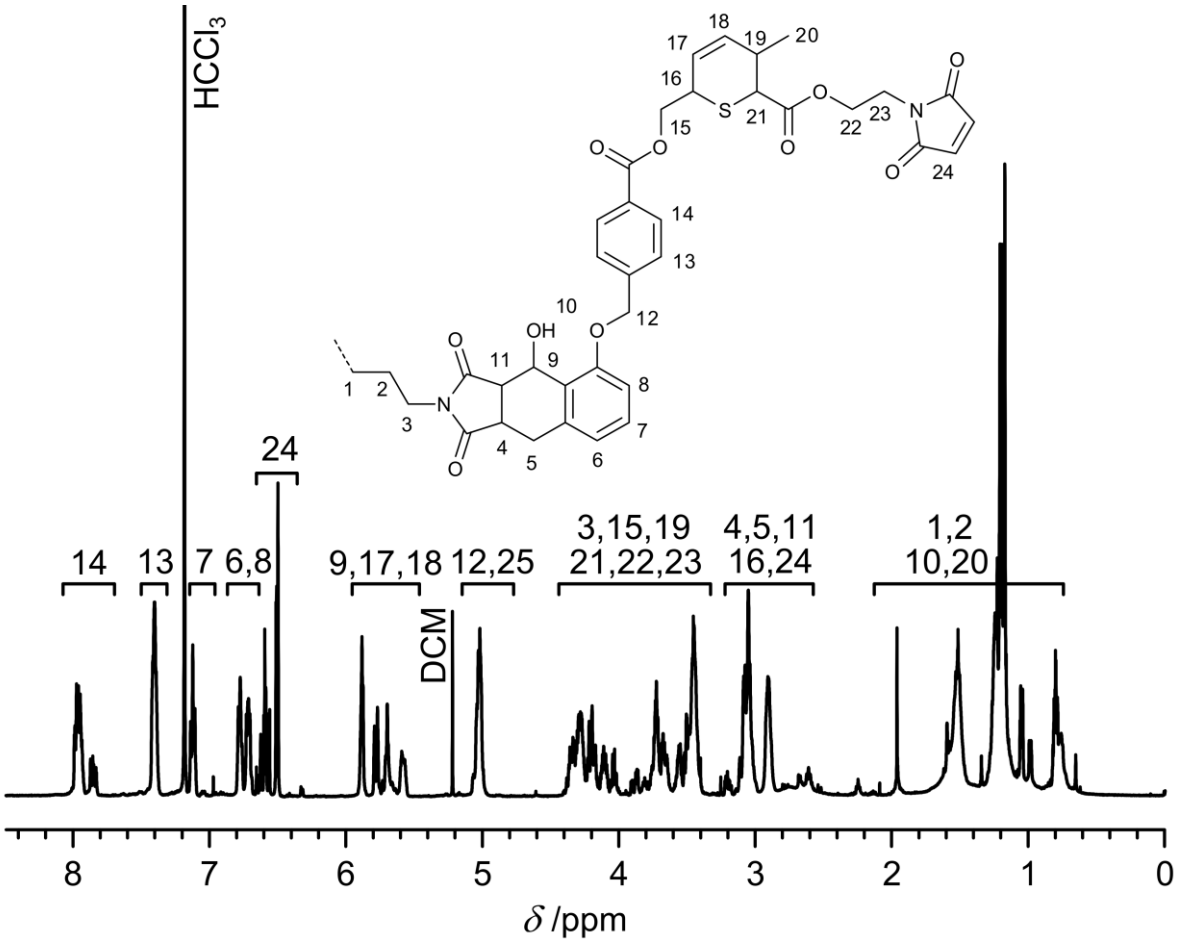

Figure S23. ^{1}H NMR spectrum of **S2d** (500 MHz, $CDCl_3$).

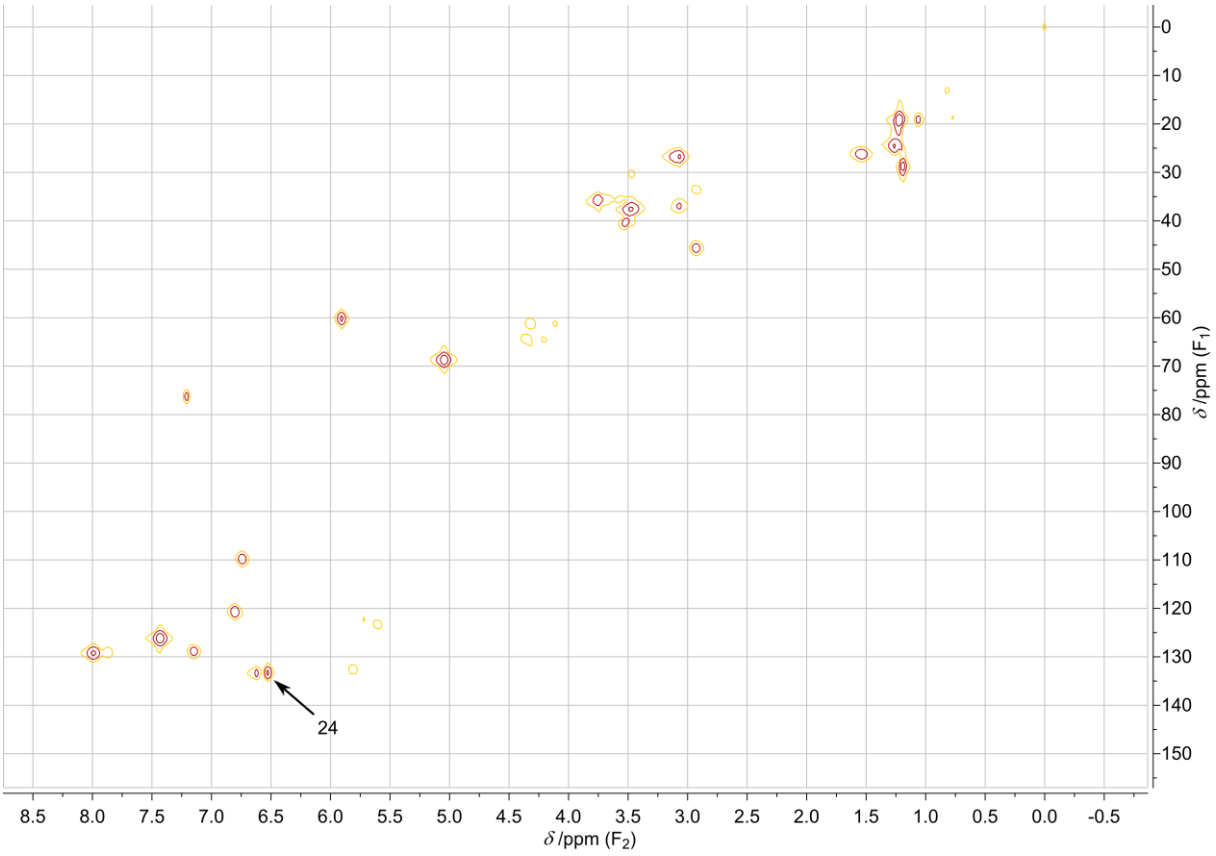

Figure S24. C-H HMQC NMR spectrum of **S2d** ($CDCl_3$). The proton *24*, representative of the furan cleavage of **S2,** is highlighted (atom assignment identical as in Table S3).

Characterization of S3

The ^{1}H NMR spectrum of **S3** enables the identification of the sorbyl end-groups, as well as the created polymer backbone, subsequent to the reaction of the maleimide end-groups from **S2d** with synthon **1**.

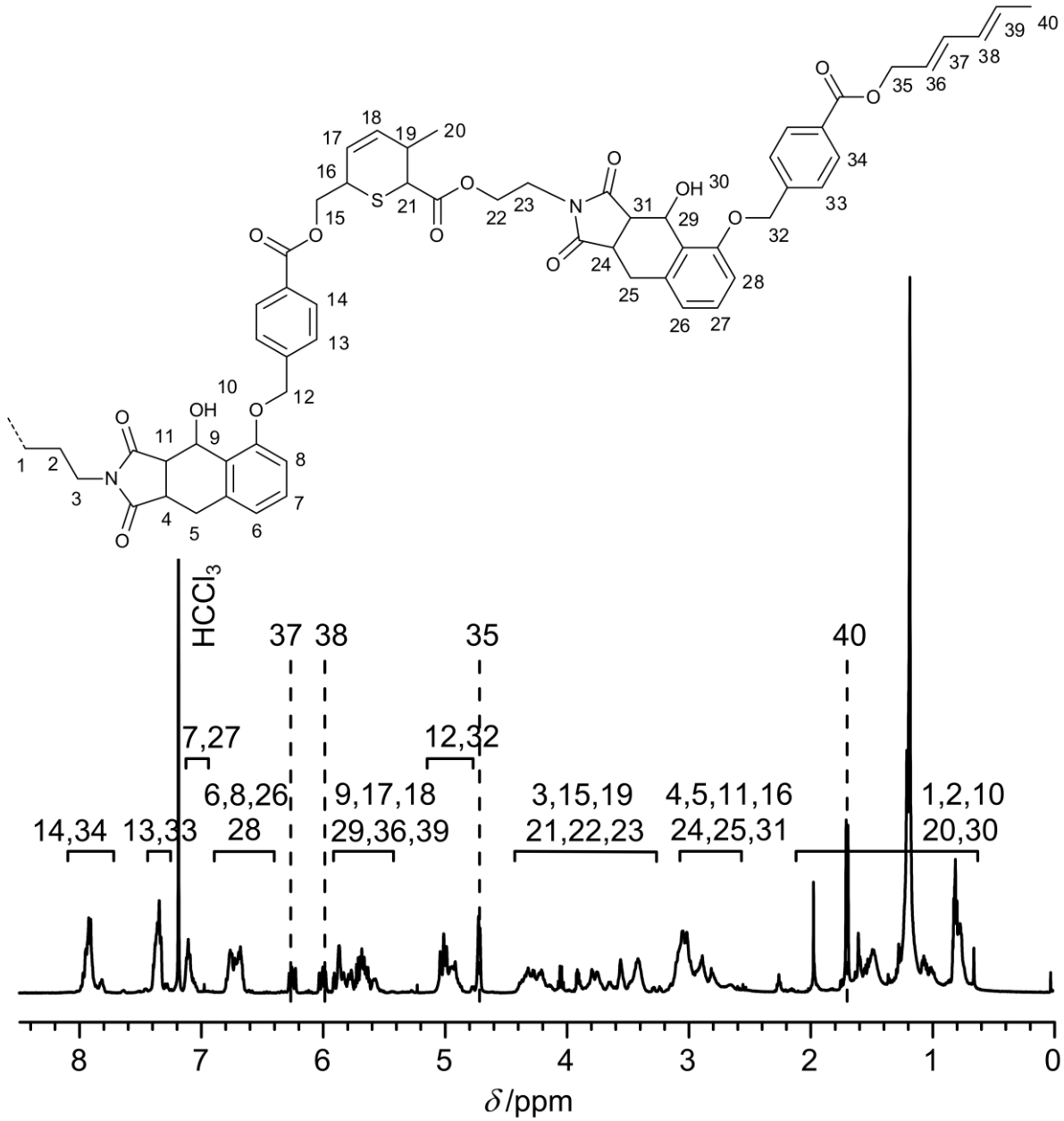

Figure S25. ^{1}H NMR spectrum of **S3** (500 MHz, $CDCl_3$).

Characterization of S4

The ^{1}H NMR spectrum of **S4** enables the identification of the furan protected maleimide end-groups, as well as the created polymer backbone, subsequent to the reaction of the sorbyl end-groups from **S3** with synthon **2**.

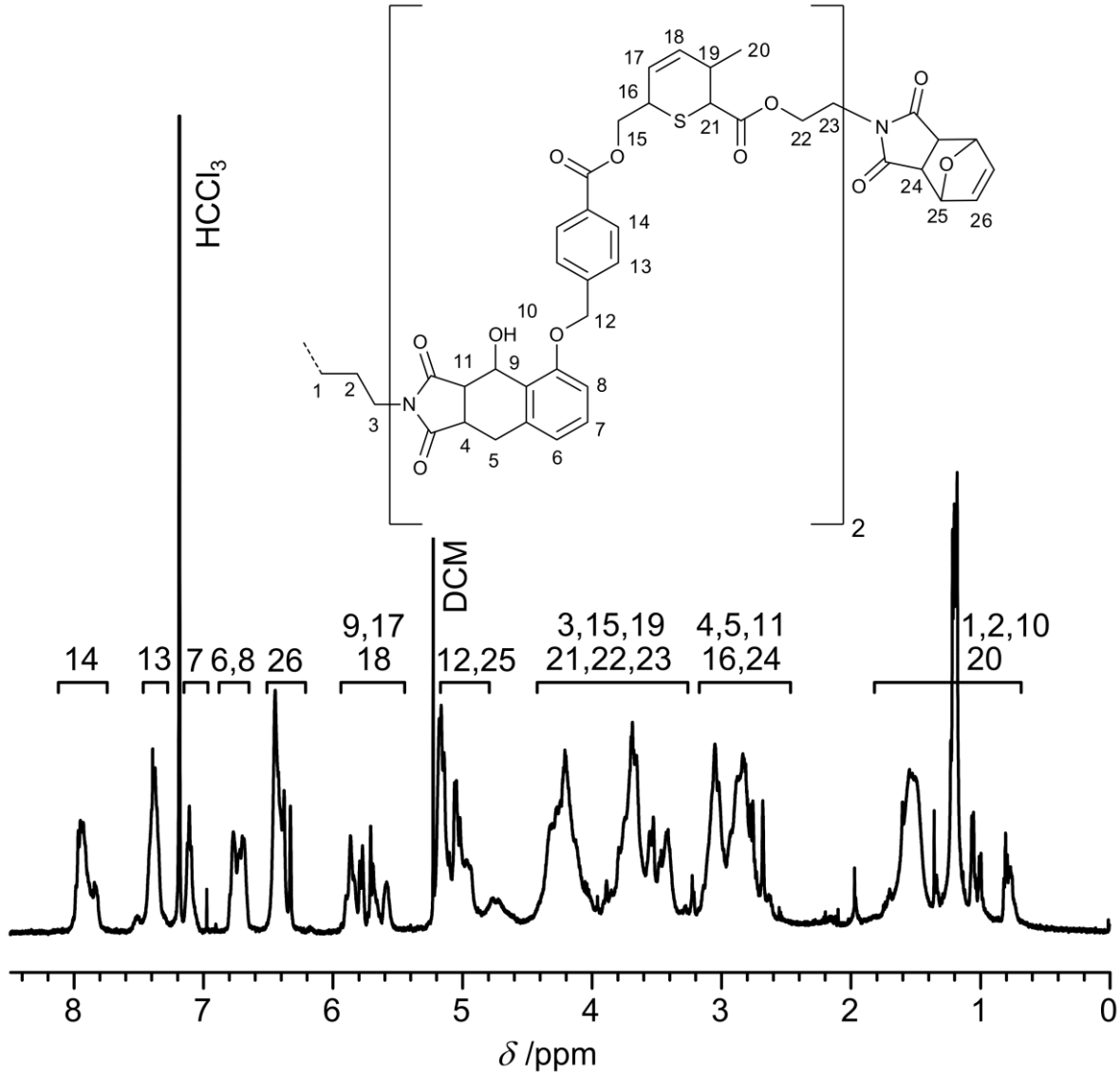

Figure S26. ^{1}H NMR spectrum of **S4** (500 MHz, $CDCl_3$).

Characterization of S4d

The ^{1}H NMR spectrum of **S4d** depicts similarities with the ^{1}H NMR spectrum of **S2d**, i.e. the cleavage of the furan moiety.

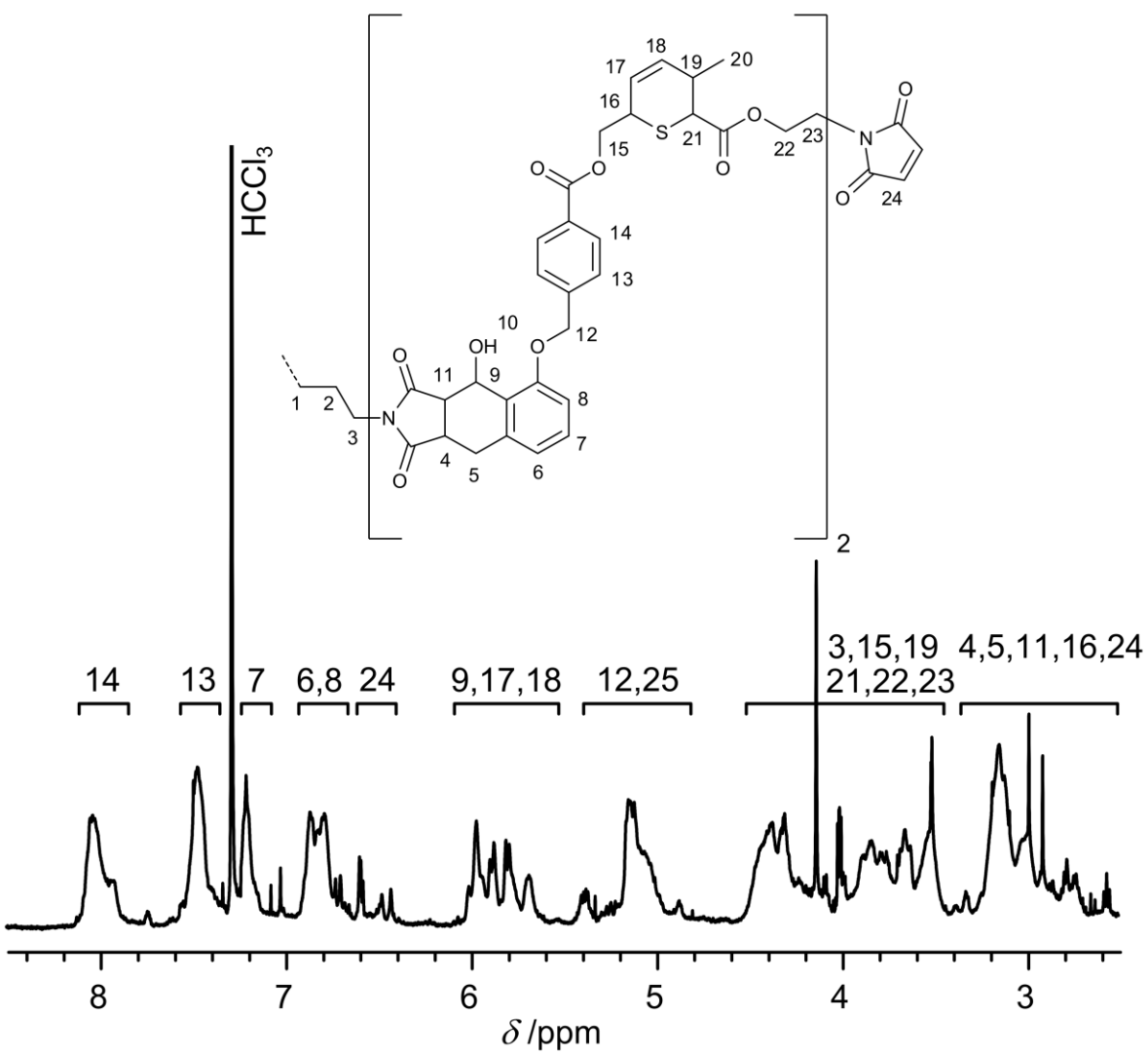

Figure S27. ^{1}H NMR spectrum of **S4d** (500 MHz, $CDCl_3$).

Characterization of S5

The ^{1}H NMR spectrum of **S5** enables the identification of the sorbyl end-groups, as well as the created polymer backbone, subsequent to the reaction of the maleimide end-groups of **S4d** with synthon **1**.

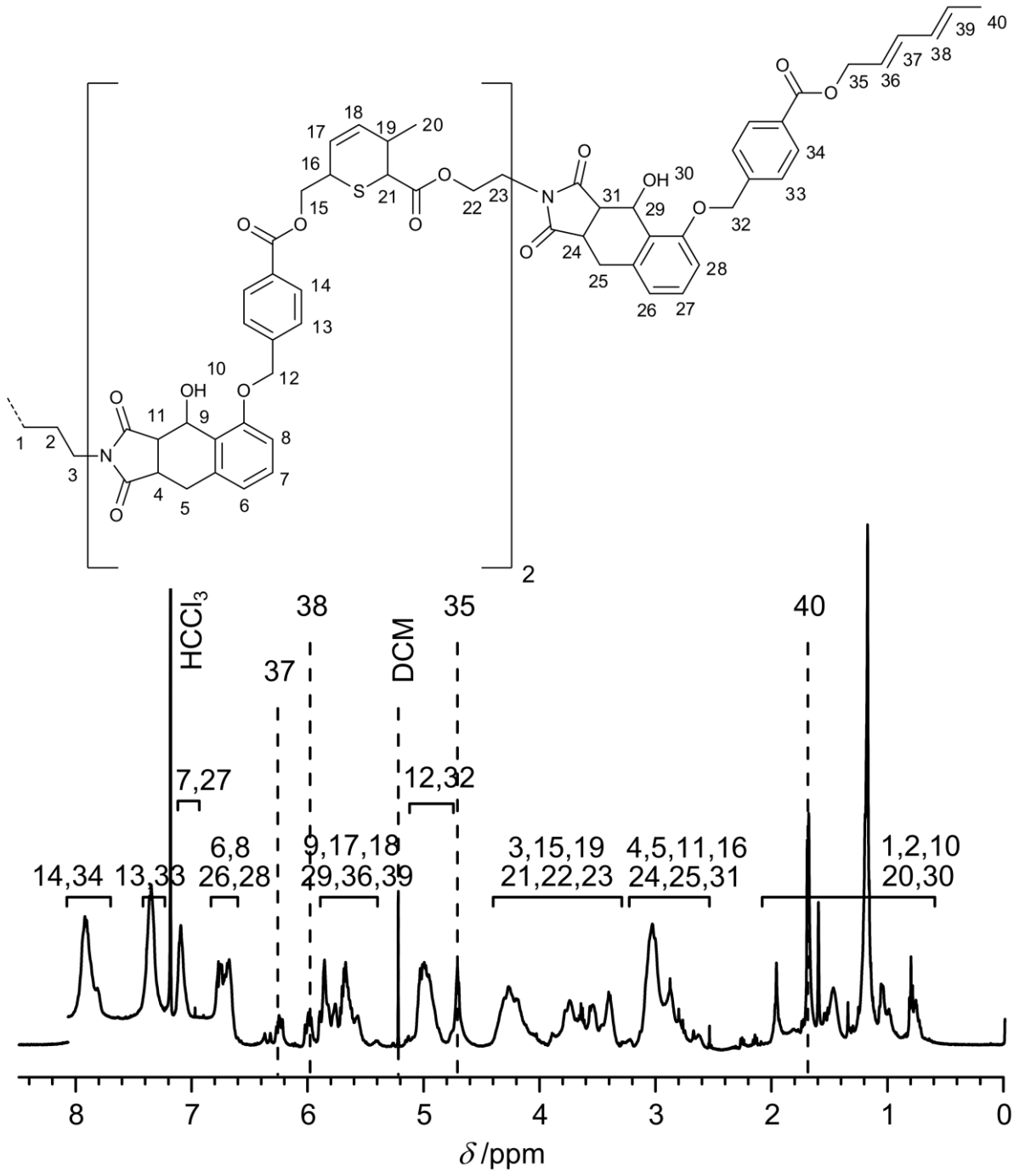

Figure S28. ^{1}H NMR spectrum of **S5** (500 MHz, $CDCl_3$).

ESI-MS

CID experiments of **S1** and **S2**

The ESI-MS spectrum after Collision Induced Decay (CID) of **S1** (Figure S29a) depicts the loss of the one sorbyl group (80.06 *m*/*z* for the fragment **S1a** at 919.42 *m*/*z*) and of a second sorbyl group (160.06 *m*/*z* for the fragment **S1b** at 839.42 *m*/*z*). Similarly, CID experiments on **S2** enabled to recognize the nature of the end-groups, with the cleavage of the one furan molecule (68.15 *m*/*z* for the fragment **S2a** at 1493.17 *m*/*z*) and of a second furan molecule (135.99 *m*/*z* for the fragment **S2b** at 1425.33 *m*/*z*, refer to Figure S29b). The fragmentation of **S2** leads to the generation of 3 additional fragments, identified as **S1**, **S1a** and **S2b**. These results are in complete agreement with the molecular structures shown in Figure S30 and S31, proving the bifunctionality of **S1** and **S2**. The summary of these results are collated and compared with predictable values in Table S4.

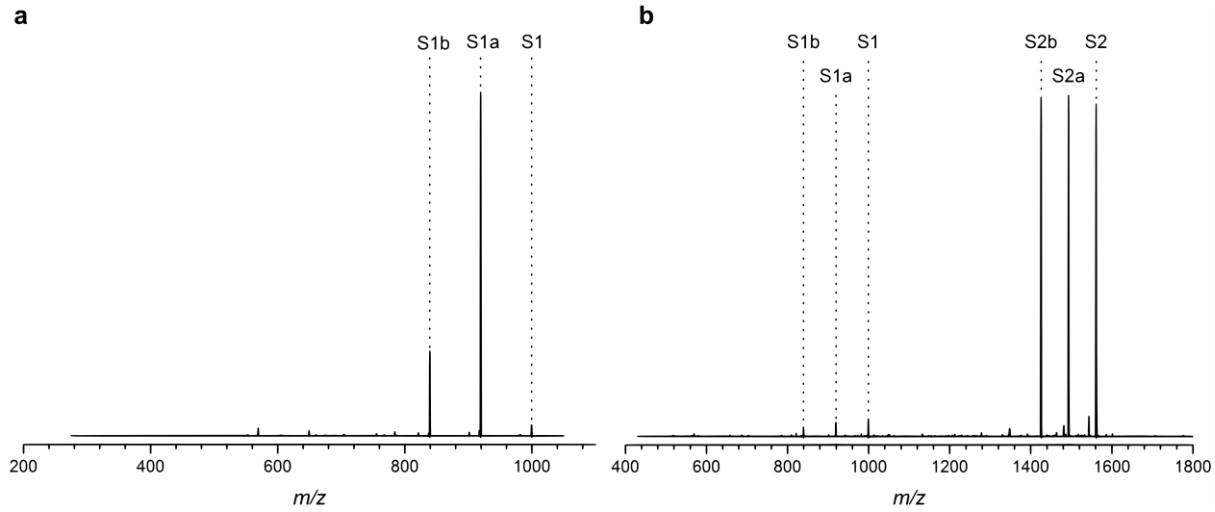

Figure S29. ESI-MS spectra after CID of **S1** (a) and **S2** (b) with the identification of the fragments **S1a**, **S1b**, **S2a** and **S2b** (solvent A conditions, sodium adducts).

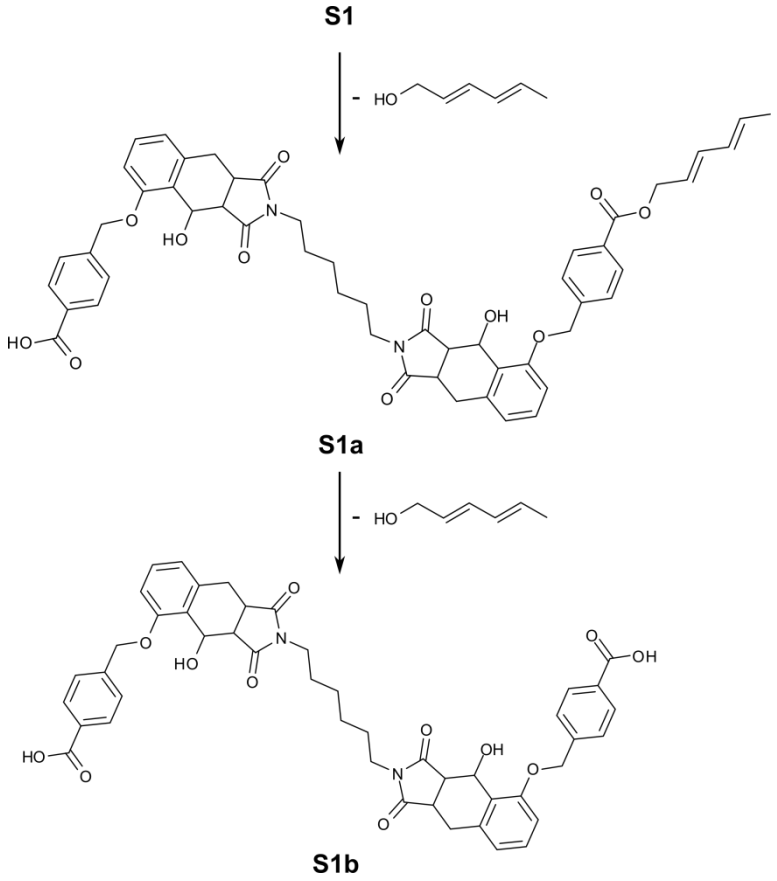

Figure S30. ESI-MS observed species during the CID experiments of **S1** and **S2** (solvent A, sodium adducts).

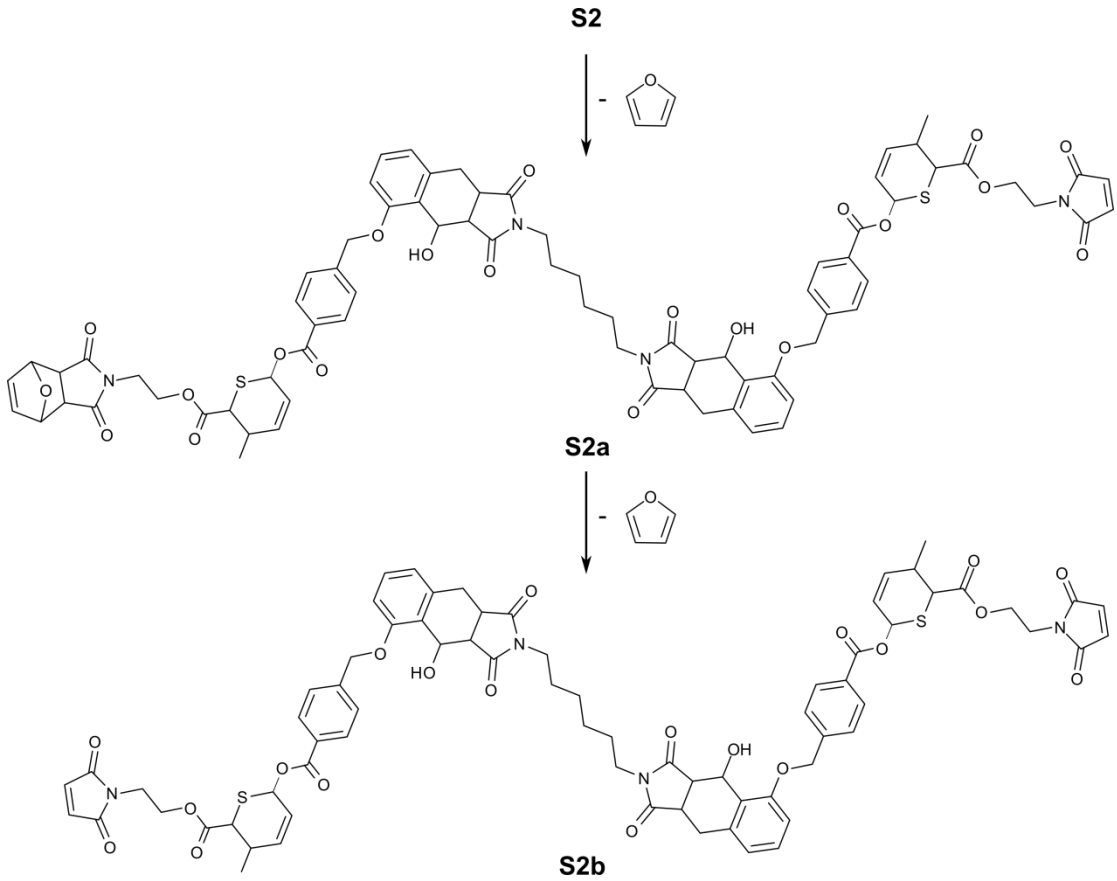

Figure S31. ESI-MS observed species during the CID experiments of **S2** (solvent A, sodium adducts).

Table S4. Comparison of the theoretical values and the experimental data obtained from ESI-MS for each synthon and the sequential products **S1** and **S2**, as sodium adducts. The fragments obtained after Collision Induced Decay (CID) experiment for **S1** and **S2** are indexed **a** and **b**. All compounds were measured with solvent A.

Species	Formula	m/z^{theo}	m/z^{exp}	$\Delta m/z$
1	$[C_{22}H_{22}O_4Na]^+$	373.14	373.20	0.06
1-1	$[C_{44}H_{43}O_8Na]^+$	722.29	722.94	0.65
2	$[C_{20}H_{19}NO_6SNa]^+$	424.08	424.10	0.02
2-2	$[C_{40}H_{38}N_2O_{12}S_2Na]^+$	825.18	824.53	0.65
core	$[C_{14}H_{16}N_2O_4Na]^+$	299.10	299.16	0.06
S1	$[C_{58}H_{60}N_2O_{12}Na]^+$	999.40	999.48	0.08
S1a	$[C_{52}H_{52}N_2O_{12}Na]^+$	919.34	919.42	0.08
S1b	$[C_{46}H_{44}N_2O_{12}Na]^+$	839.28	839.42	0.14
S2	$[C_{82}H_{82}N_4O_{22}S_2Na]^+$	1561.48	1561.32	0.16
S2a	$[C_{78}H_{78}N_4O_{21}S_2Na]^+$	1493.45	1493.17	0.28
S2b	$[C_{74}H_{74}N_4O_20S_2Na]^+$	1425.42	1425.33	0.09

Detailed spectra of **S1**, **S2** and **S3**

The detailed ESI-MS spectra of **S1**, **S2** and **S3** reported in the main text (Figure 5) measured in solvent B (CTA adducts) are depicted in Figure S32. For each compound, the predictable spectrum is represented below the experimental spectrum. Table S5 enables to draw a comparison between the theoretical and the experimental values.

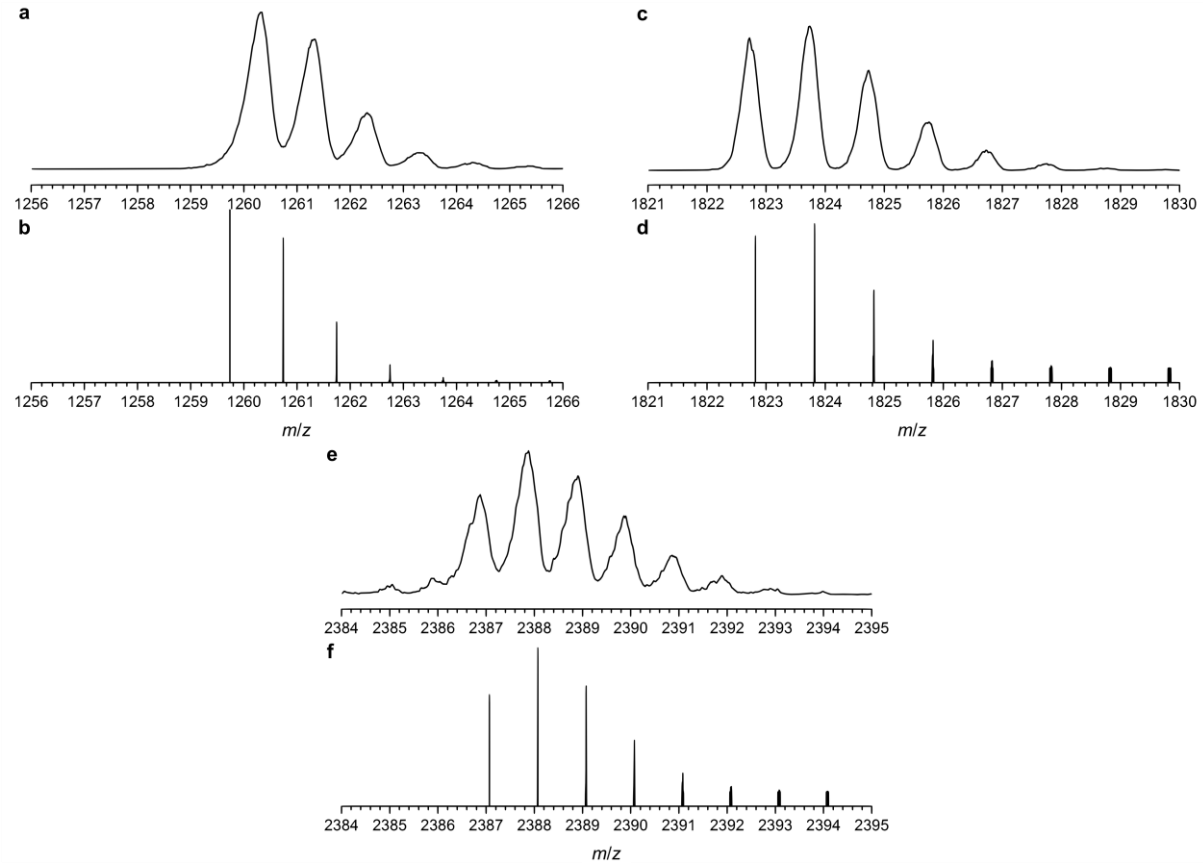

Figure S32. ESI-MS spectra of **S1** (a), **S2** (c) and **S3** (e) measured under solvent B conditions (CTA adducts). For each compound, the predictable spectrum is represented below the experimental spectrum, (b) for **S1**, (d) for **S2** and (f) for **S3**.

Table S5. Comparison of the theoretical values and the experimental data obtained from ESI-MS for each sequential compound **S1** to **S3** measured with solvent B (CTA adducts).

Species	Formula	m/z^{theo}	m/z^{exp}	$\Delta m/z$
S1	$[C_{77}H_{102}N_3O_{12}]^+$	1260.75	1260.34	0.59
S2	$[C_{101}H_{124}N_5O_{22}S_2]^+$	1822.82	1822.72	0.1
S3	$[C_{137}H_{160}N_5O_{28}S_2]^+$	2387.07	2386.86	0.21

MALDI-TOF-MS of S5

Table S6. Comparison of the theoretical values and the experimental data obtained from MALDI-TOF-MS for **S5** from the DIT matrix (sodium adducts). The difference between the calculated and experimental value ($\Delta m/z$) is higher than measurements performed via ESI-MS, and can be caused by a protonation during the ionization.

Species	Formula	m/z^{theo}	m/z^{exp}	$\Delta m/z$
S5	$[C_{178}H_{176}N_6O_{44}S_4Na]^+$	3253.05	3257.01	3.96

SEC traces of S2d and S4d

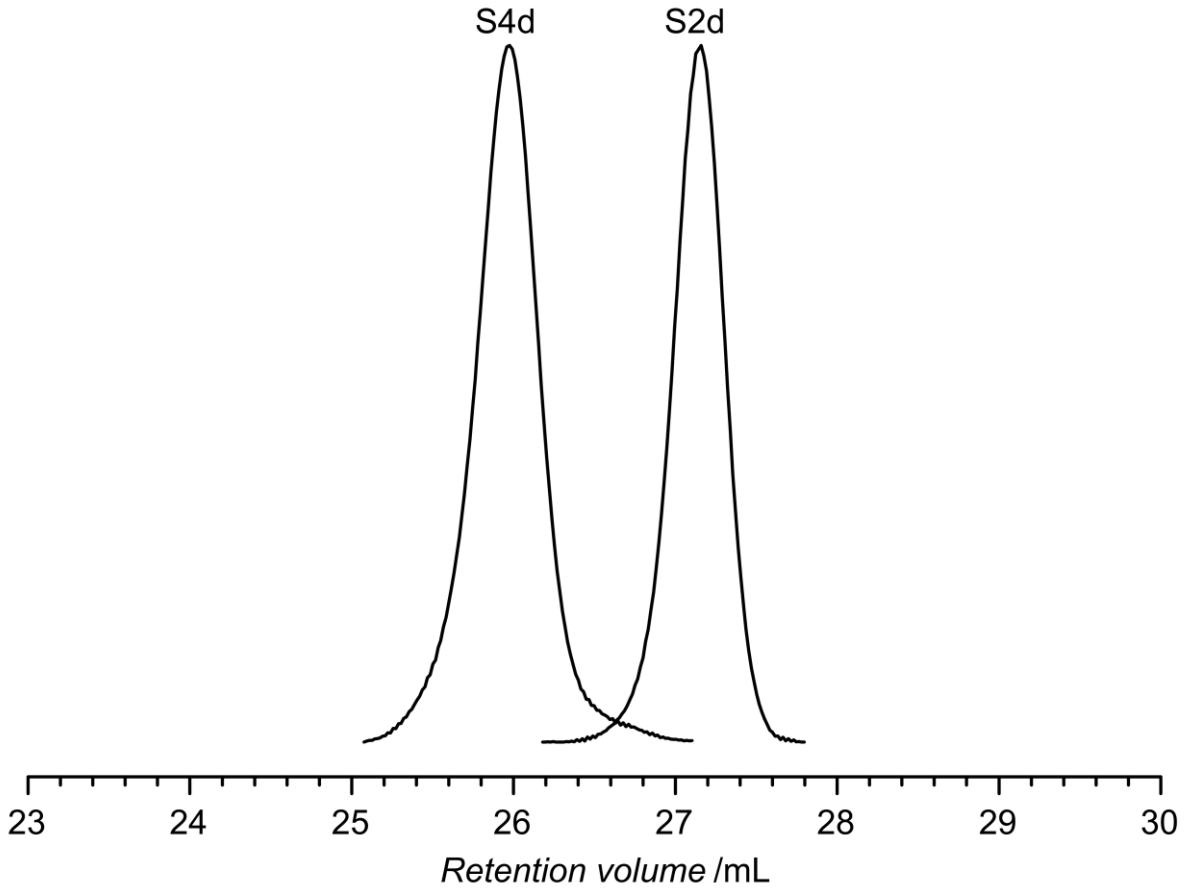

Figure S33. SEC traces of **S2d** (M_n = 1350 Da, M^{theo} = 1403.52 Da, $Đ$ = 1.01) and **S4d** (M_n = 2500 g·mol^{-1}, M^{theo} = 2530.76 Da, $Đ$ = 1.01) after the furan cleavage of **S2** and **S4**, respectively. SEC traces recorded in THF (PS calibration).

References and Notes

[1] K. Oehlenschlaeger, J. O. Mueller, N. B. Heine, M. Glassner, N. K. Guimard, G. Delaittre, F. G. Schmidt, C. Barner-Kowollik, *Angew. Chem. Int. Ed.* **2013**, *52*, 762-766.

[2] W. M. Gramlich, M. L. Robertson, M. A. Hillmyer, *Macromolecules* **2010**, *43*, 2313-2321.

[3] E. Vedejs, T. H. Eberlin, R. G. Wilde, *J. Org. Chem.* **1988**, *53*, 2220-2226.

[4] J. Canadell, H. Fischer, G. De With, R. A. T. M. Van Benthem, *J. Polym. Sci. A Polym. Chem.* **2010**, *48*, 3456-3467.

[5] T. Dispinar, W. Van Camp, L. J. De Cock, B. G. De Geest, F. E. Du Prez, *Macromol. Biosci.* **2012**, *12*, 383-394.